DOI 10.1002/pmic.200401351 *Proteomics* 2006, *6*, 2504–2529

RESEARCH ARTICLE

Proteomic analyses of *Oryza sativa* mature pollen reveal novel proteins associated with pollen germination and tube growth

Shaojun Dai[1], *Lei Li*[1], *Taotao Chen*[1], *Kang Chong*[1], *Yongbiao Xue*[2], *Tai Wang*[1]

[1] Key Laboratory of Photosynthesis & Environmental Molecular Physiology, Research Center for Molecular & Developmental Biology, Institute of Botany, Chinese Academy of Sciences, Beijing, P. R. China
[2] Key Laboratory of Molecular & Developmental Biology, Institute of Genetics and Developmental Biology, Chinese Academy of Sciences, Beijing, P. R. China

As a highly reduced organism, pollen performs specialized functions to generate and carry sperm into the ovule by its polarily growing pollen tube. Yet the molecular genetic basis of these functions is poorly understood. Here, we identified 322 unique proteins, most of which were not reported previously to be in pollen, from mature pollen of *Oryza sativa* L. ssp *japonica* using a proteomic approach, 23% of them having more than one isoform. Functional classification reveals that an over-representation of the proteins was related to signal transduction (10%), wall remodeling and metabolism (11%), and protein synthesis, assembly and degradation (14%), as well as carbohydrate and energy metabolism (25%). Further, 11% of the identified proteins are functionally unknown and do not contain any conserved domain associated with known activities. These analyses also identified 5 novel proteins by *de novo* sequencing and revealed several important proteins, mainly involved in signal transduction (such as protein kinases, receptor kinase-interacting proteins, guanosine 5'-diphosphate dissociation inhibitors, C2 domain-containing proteins, cyclophilins), protein synthesis, assembly and degradation (such as prohibitin, mitochondrial processing peptidase, putative UFD1, AAA^+ ATPase), and wall remodeling and metabolism (such as reversibly glycosylated polypeptides, cellulose synthase-like OsCsLF7). The study is the first close investigation, to our knowledge, of protein complement in mature pollen, and presents useful molecular information at the protein level to further understand the mechanisms underlying pollen germination and tube growth.

Received: June 15, 2004
Revised: July 29, 2005
Accepted: September 27, 2005

Keywords:
Mass spectrometry / Mature pollen / *Oryza sativa* L.

Correspondence: Dr. Tai Wang, Key Laboratory of Photosynthesis & Environmental Molecular Physiology, Research Center for Molecular & Developmental Biology, Institute of Botany, Chinese Academy of Sciences, 20 Nanxincun, Xiangshan, Haidianqu, Beijing 100093, P. R. China
E-mail: twang@ibcas.ac.cn
Fax: +86-10-62594170

Abbreviations: ARG1, altered response to gravity; **CBL**, calcineurin B-like protein; **CC-NBS-LRR**, N-terminal coiled-coil motif, nucleotide-binding site and C-terminal leucine-rich repeat domains; **CIPK**, CBL-interacting protein kinase; **GDI,** GDP dissociation inhibitors; **GDP**, guanosine diphosphate; **GTP**, guanosine triphosphate; **NP-40**, Nonidet P-40 detergent; DAPI, 4',6-diamidino-2-phenylindole; **PIP**, pollen-interior protein; **PRP**, pollen-released protein; **SnRK1b**, sucrose non-fermenting 1-related protein kinase; **UDP**, uridine diphosphate; **ULP1**, ubiquitin-like protein 1

1 Introduction

In flowering plants, the highly specialized haploid male plant (pollen or male gametophyte) generated from diploid microsporocytes in anthers of stamen is a key regulator of sexual reproduction and contributes to selection of vigorous offspring and genetic diversity of population. Biochemical and physiological analyses have revealed that mature pollen grains contain presynthesized proteins and mRNAs. The presynthesized proteins are required for pollen germination, and new protein synthesis is required only for the growth of the pollen tube following germination [1]. Therefore, mature pollen might have all the proteins involved in its functional specialization leading to fertilization in early fertilization events, including hydration, cohesion, establishment of pollen tube

polarity and cell recognition of pollen-stigma, and initiation of a hierarchical signal cascade. Recently, several proteins identified in the mature pollen of some species have been shown to be involved in hydration, cohesion and cell recognition of pollen-stigma [2–4]. The importance of tip-focused intracellular Ca^{2+} and tip plasma membrane-localized Rop1 GTPase in polar establishment of pollen tubes and tube growth is well understood [5, 6], but little biochemical and molecular genetic information exists on pollen functions.

Some recent studies have tried to break the bottleneck. Transcriptomic analyses of Arabidopsis pollen have identified some transcripts expressed preferentially in pollen [7,8]. Functional classification revealed that most of these deduced proteins encoded by mRNAs expressed preferentially in pollen are involved in cell wall biosynthesis, cytoskeleton and signal transduction [7, 8], which indicates that these cellular processes play a vital role in pollen development and function. But increasing data show the lack of a simple correlation between the transcriptional profile and protein complement in a given cell or tissue. The popular situation in eukaryotic cells is that a gene usually gives rise to multiple protein isoforms, possibly with different functions, after alternative splicing and/or essential posttranslational modification [9]. Thus, proteomic study is essential for unraveling the biological complexity to understand pollen functions.

Compared with the quickly increasing data of pollen transcriptional profiles, our present knowledge of mature pollen proteome is inadequate. Yet it is essential for understanding the biological characterization of the highly specialized organism. Recently, studies by Mayfield *et al.* [10] and Kerim *et al.* [11] have characterized numerous proteins from Arabidopsis pollen coat and from developing rice anthers, respectively, but the protein complement of mature pollen still remains to be investigated [12].

Here, we report for the first time, to our knowledge, our analysis of the protein complement of mature pollen using 2-DE with MALDI-TOF MS and ESI Q-TOF MS/MS, and 1-D SDS PAGE with nano-LC ESI Q-TOF MS/MS. These analyses identified 322 unique proteins, most of which have not been reported previously to be in pollen. The identified proteins can be assigned into 16 distinct groups. The proteins related to carbohydrate and energy metabolism, protein synthesis, assembly and degradation, wall remodeling and metabolism, and signal transduction were overrepresented.

2 Materials and methods

2.1 Plant growth and pollen collection

Rice cultivar Zhonghua 10 (*Oryza sativa* L. ssp *japonica*) was grown under natural conditions. The plants were fertilized and flooded normally. Mature pollen grains were collected by shaking panicles gently during flowering, and were used or stored at −80°C immediately.

2.2 Observation of pollen morphology

To monitor cytological changes of pollen grains while preparing proteins, we observed morphological and cytological characteristics of mature rice pollen under a microscope (Axioskop 40 Fluorescence Microscope, Zeiss, Germany) by staining with 1% I_2-KI or 0.2 μg/μL DAPI, and under a scanning electric microscope (SEM, HITACHI S-800, Japan) after drying in air. For ultrastructure observation, pollen grains were fixed in a buffer of 3% glutaraldehyde and 2% osmic acid, and then embedded in Spurr (Sigma). The specimens were thin-sectioned using a diamond knife on a LKB-Nova ultramicrotome, mounted on a grid, and then stained with uranylacetate at 20°C for 30 min followed by lead citrate for 20 min. Finally, the stained specimens were observed under a transmission electron microscopy (TEM, JEM-1230, Japan).

2.3 Preparation of pollen-released proteins (PRPs) and pollen-interior proteins (PIPs)

To prepare pollen-released proteins (PRPs), 0.5 g of pollen grains were suspended in 5 mL elution buffer (0.7 M sucrose, 0.5 M Tris-HCl, pH 7.2, 50 mM EDTA, 10 mM KCl, 2 mM PMSF, 13 mM DTT) and incubated with gentle shaking on ice for 15 min. Eluate (containing PRPs) was collected by centrifuged at $50 \times g$ for 10 min, and the pelleted pollen grains were used in the next cycle of elution. This procedure was repeated until the proteins in the eluate were hardly detected by the Bradford method [13]. After each elution, the intactness of the eluted pollen grains was checked under microscope. The eluates were combined and then centrifuged at $18\,000 \times g$ for 20 min. The resultant supernatant was used as the PRP fraction. The PRPs were precipitated with 12.5% trichloroacetic acid on ice for 2 h, and then collected by centrifugation at $15\,000 \times g$ for 20 min at 4°C. The pelleted PRPs were resuspended in 80% cold acetone containing 0.07% β-mercaptoethanol, cooled at −20°C for 30 min, and finally collected by centrifuged at $15\,000 \times g$ for 20 min at 4°C. After being rinsed with cold acetone with 0.07% β-mercaptoethanol and dried by vacuum, the resultant proteins were dissolved in protein lysis buffer (7 M urea, 2 M thiourea, 4% v/v NP-40, 13 mM DTT, 2% v/v pharmalyte 3–10) and used for 2-DE immediately or stored at −80°C after debris was removed by centrifugation at $20\,000 \times g$ for 20 min at 4°C.

The eluted pollen grains, used to extract pollen-interior proteins (PIPs), were homogenized in a homogenate buffer (100 mM Tris-HCl pH 7.6, 5 mM KCl, 2% SDS, 2% NP-40, 1% β-mercaptoethanol) with chilled mortar and pestle. After almost all pollen grains were broken (confirmed by microscopy), the homogenate was centrifuged at $18\,000 \times g$ for 20 min and the resultant supernatant was used for preparation of PIPs by the same procedure described above. Protein concentrations were determined according to the Bradford method [13] by DU640 UV-visible spectrophotometry (Beckman). BSA was used as the standard.

2.4 Fraction of pollen coat-associated proteins

To collect pollen coat-associated proteins, the freshly collected mature pollen grains (100 mg) were eluted by 500 μL diethyl ether for about 1 min, and centrifuged at 500 × *g*. The collected supernatant was vaporized by SpeedVec (ThermoSavant), resolved by SDS sample buffer (50 mM Tris-HCl, pH 6.8, 100 mM DTT, 2% SDS, 10% glycerol, 0.1% bromophenol blue), and then subjected to standard 1-DE with 12.5% SDS polyacrylamide gel. The resulting gel was briefly stained by CBB G250, and the detected protein bands were cut into horizontal slices (14 in total). Gel slices were digested and processed as described in Section 2.7.

2.5 2-DE, gel staining and image analysis

An aliquot (about 600 μg proteins) of PRP or PIP sample was diluted with rehydration buffer (7 M urea, 2 M thiourea, 1% v/v NP-40, 13 mM DTT, 0.5% IPG Buffer 3–10, 0.002% Bromophenol Blue), loaded onto an IPG strip holder with 24 cm, pH 3–10 or pH 4–7 linear gradient IPG strips (Amersham Biosciences, Sweden) and was run in an Ettan IPGphor Isoelectric Focusing System following the protocol of the manufacturer. For SDS-PAGE, the equilibrated IPG gel strips were placed onto 12.5% ExcelGel SDS gels (Amersham Pharmacia Biotech) using an Ettan DALT Six Electrophoresis Unit. Low molecular-mass (MM) protein markers (Fermentas, Canada) were co-electrophoresed and used as MM standards. The proteins in gels were visualized by CBB staining. The experiments were repeated 3 times for each preparation of PRPs and PIPs.

2-DE Images were obtained by scanning each stained gel at 300 dots *per* inch resolution using an ImageScanner (Amersham Bioscience, Sweden) and analyzed using ImageMaster 2D 2002.01 software. The apparent MM of each protein in gel was determined with the co-electrophoresized low MM protein markers as standards, and the apparent isoelectric point (p*I*) of each protein was determined by its migration on IPG linear strips using the analysis program.

2.6 MALDI-TOF MS and ESI Q-TOF MS/MS

The visualized protein spots were excised from 2-DE gels by Ettain Spot Cutter (Amersham Bioscience, Sweden). Each spot was destained in a destaining buffer [25 mM ammonium bicarbonate, 50% v/v ACN], dehydrated by ACN and spun-dry, and digested in-gel with sequencing grade modified trypsin (Roche) (10 ng/μL in 25 mM ammonium bicarbonate) for 16 h at 37°C.

For protein identification by MALDI-TOF MS, one aliquot of the enzyme digest solution was spotted onto a sample plate with matrix (α-cyano-4-hydroxcinnamic acid, 8 mg/mL in 50% v/v TFA) and allowed to air dry. MALDI-TOF MS involved use of the Autoflex MALDI mass spectrometer (Bruker Daltonics, Germany), equipped with a flight tube (reflex mode, 2.6 m long), laser (N2, 337 nm) and scout 384 target system. The accelerating voltage was 20 kV and the microchannel plate (MCP) detector worked at 1.6 kV. Mass spectra were acquired in a positive mode. Known trypsin autocleavable peptide masses (906.51 and 2273.16 DA) were used for a 2-point internal calibration for each spectrum. PMFs were searched against NCBI protein databases with the search engine Matrix Science at http://www.matrixscience.com. *Oryza sativa* was chosen for the taxonomic category. All peptide masses were assumed to be monoisotopic and $[M+H]^+$ (protonated molecularions). Searches were conducted using a mass accuracy of ±100 ppm, and 1 missed cleavage site was allowed for each search.

The protein spots, which could not be identified by PMF search in NCBI database, were subjected to nanospray ESI Q-TOF MS/MS (Micromass). Before loading the digested peptide samples, the instrument accuracy was calibrated by the external calibration of Glu-Fib (3 ppm). About 1–2 μL of the sample was desalted with a trapping column and loaded in the Nanoflow Probe Tip (Micromass). The applied spray voltage was 800–1000 V, with a sample cone working on 25–40 V. The MCP detector working voltage was 2250 V, and energy adjustable collision cell was filled with pure argon gas. MS/MS data were processed using MassLynx 3.5 and searched against NCBInr protein sequence databases with the MS/MS ion searching program MASCOT (http://www.matrixscience.com).

2.7 nano-LC ESI Q-TOF MS/MS

Sliced 14 protein bands from 1-DE gels were destained and digested as described in Section 2.6. Each peptide mixture was dissolved in 3 μL of 0.1% TFA and 2% ACN, and injected by autosampler into a 0.3 × 1 mm trapping column (PepMap C18; LC Packings) by means of a CapLC system. Peptides were eluted into a Q-TOF mass spectrometer (Q-TOF Micro; Micromass) at 200 nL/min on a C18 column (75 μm × 15 cm; LC Packings). The mobile phase A was water/ACN (95/5, v/v) with 0.1% TFA, the mobile phase B water/ACN (5/95, v/v) with 0.1% TFA, and the flow rate 3.0 μL/min. The nonlinear gradient was set as 10%–90% B in 60 min, 90%–100% B in 5 min and retaining 100% B for 5 min, and then reaching 100% A in 5 min. The MS/MS data were processed and searched as described above.

2.8 Western blot analysis

After separation on 1-DE with 12.5% SDS polyacrylamide gel or 2-DE with pH 4–7 linear gradients IPG strips (Amersham Biosciences, Sweden), the proteins were electrophoretically transferred on a semidry blot apparatus to a polyvinylidene difluoride (PVDF) membrane (Pierce) with a buffer of 10 mM 3-cyclohexylamino-1-propanesulfonic acid (CAPS) and 10% v/v methanol at 2-mA constant current *per* cm^2 gel for 1 h. For immunodetection, the membranes were blocked for 2 h with 5% skimmed milk w/v in Tris-HCl (pH 7.5) buffered saline containing 150 mM NaCl, incubated for 2 h

with the same buffer containing primary rabbit antibody, washed with Tris-HCl (pH 7.5) buffered saline containing 0.05% v/v Tween 20 and 150 mM NaCl, and Tris/HCl (pH 7.5) buffered saline containing 150 mM NaCl, and then incubated for 1 h with goat anti-rabbit IgG-conjugated alkaline phosphatase conjugate (1:2000 dilution, Sino-Amico). The hybridized membrane was washed, and positive signals were visualized using 0.1 mg/mL 5-bromo-4-chloro-3-indolyl phosphate and 0.2 mg/mL nitroblue tetrazolium (Sigma Corp) in a buffer of 100 mM Tris-HCl pH 9.5, 100 mM NaCl and 5 mM $MgCl_2$.

3 Results and discussion

3.1 Cytological characters of mature rice pollen grains

The structural characteristics of pollen are very important for its longevity. Like the pollen grains of other cereals that have thin walls, mature rice pollen grains can live only for about 5 min after being released from anthers under natural conditions [14], which may explain the few molecular studies on pollen from cereal species except maize [15]. Here, we characterized the microstructure and ultrastructure of mature rice pollen under light microscopy, SEM and TEM. Mature rice pollen is a tricellular organism (Fig. 1A) and has abundant mitochondria, endoplasmic reticulum and vesicles (Fig. 1E and F) as well as abundant starch granules. The pollen grains are spherical (diameter is about 38–42 μm) with a single operculate aperture (Fig. 1B and C). The diameter of the aperture and opercle is about 3.5–4.0 μm and 2.1–2.4 μm (Fig. 1C), respectively. The exine, which is about 0.7 μm wide and interspersed with granules (Fig. 1D), is composed of tectum (0.15–0.25 μm), columellae (0.2 μm) and the foot layer (0.15–0.25 μm thick). Plentiful microchannels, with a diameter of about 0.02–0.03 μm, are present in both the tectum and foot layer (Fig. 1D). The intine is not uniformly thick (about 0.2–0.4 μm) with relatively high electron density (Fig. 1D). Therefore, the rice pollen wall (0.8–1.2 μm thick) is thinner than that of the pollen of other cereals such as maize whose pollen wall is 1.3–1.5 μm thick [16]. Probably the thinner and porous wall with many microchannels is related to the release of proteins during cell-cell recognition of pollen-stigma. But the abundant microchannels in the exine also result in rapid water loss. This explains why it is difficult to store mature rice pollen grains.

3.2 Identification of 2-DE spots by MALDI-TOF MS and ESI Q-TOF MS/MS

Pollen extracellular matrices contain a set of proteins, which are proposed to mediate efficient pollination and fertilization by hydrolyzing and remodeling the cell wall in the stigma and transmitting tract of a style, and to signal the interaction of pollen-stigma [10], but the information about these proteins is

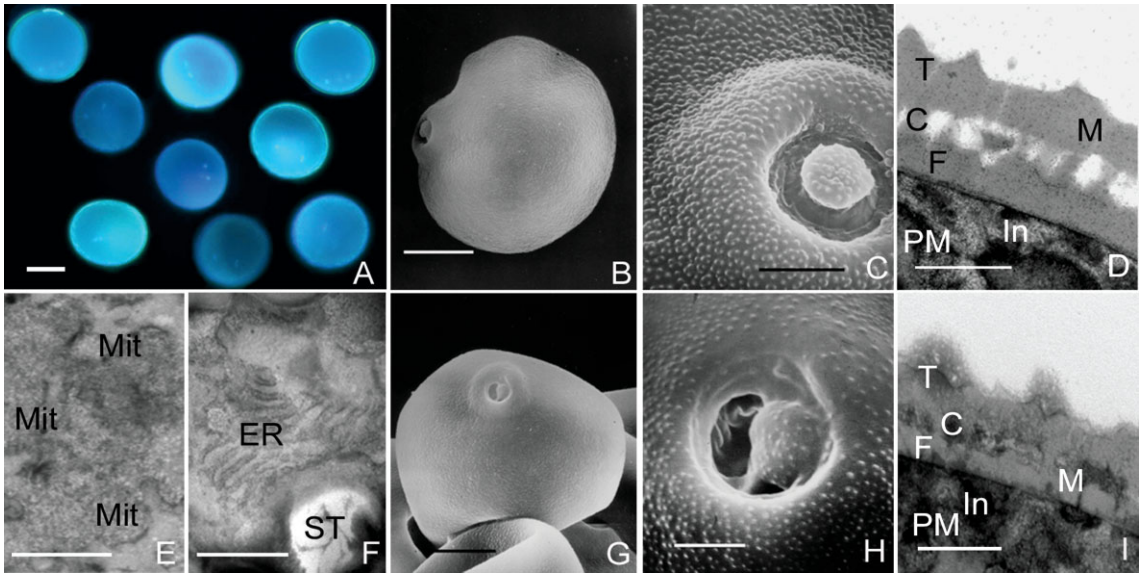

Figure 1. Cytological observation of fresh mature pollen and eluted mature pollen. A~F, fresh mature pollen: A, tricellular fresh pollen grains stained by DAPI, bar = 20 μm; B, an equatorial view under SEM, bar = 12 μm; C, aperture under SEM, bar = 3 μm; D, wall ultrastructure under TEM, bar = 0.25 μm; E and F, show abundant Mits and ERs under TEM, bar = 0.75 μm. G~I, eluted mature pollen: G, an polar view, bar = 15 μm; H, shows a ruptured aperture, bar = 3 μm; I, wall ultrastructure shows the substances with higher electron density in microchannels and columellae and illegible outer edge of the extine, bar = 0.17 μm.
T, tectum; C, columellae; F, foot layer; M, microchannel; In, intine; PM, plasma membrane; ST, starch granules; ER, endoplasmic reticulum; Mit, mitochrondria.

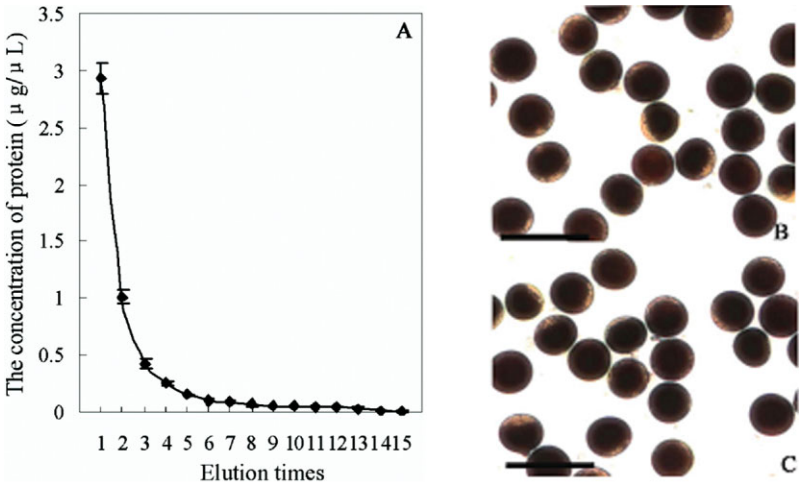

Figure 2. Protein concentrations in each eluate (A) and the I_2-KI reaction of pollen (B and C, bar = 80 μm) during PRP preparation. A, 0.5 g of fresh pollen was eluted in an isotonic buffer on ice. Eluate was collected by centrifuge at $50 \times g$; pelleted pollen grains were used in the next cycle of elution. After 15 cycles of elution, the protein concentration in eluate was hardly detected by the Bradford method. The eluates contain the PRPs (also see Section 2). B, fresh pollen grains stained by I_2-KI. C, eluted pollen grains stained by I_2-KI.

currently very limited [12]. To identify the extracellular proteins and gain an insight into protein complement of pollen, we applied a two-step procedure to fractionate pollen proteins into PRPs and PIPs by eluting mature pollen grains in an isotonic buffer (see Section 2). This elution process was monitored by determining the protein concentration of each eluate, which was 2.92 μg/μL in the first eluate and decreased to lower than 0.04 μg/μL in the last eluate (Fig. 2A).

The eluted pollen grains had normal I_2-KI reaction and cell morphology (Fig. 2C) compared with fresh pollen grains (Fig. 2B), and only about 5% of them burst. They had a normal wall surface structure with some having ruptured apertures as seen under SEM (Fig. 1G and H). Furthermore, we evaluated the efficiency of this procedure in enriched PRPs by Western blot analysis. 1-DE-Separated PRPs and PIPs were detected by antibodies against beta-1,4-xylanase, a representative pollen coat protein identified in maize [15], plasma membrane (PM) H^+-ATPase PMA2 from *Nicotiana plumbaginifolia* [17] and rice OsRad21-3 (AY371048), a nucleus-localizing protein [18]. The beta-1,4-xylanase homolog was most abundant in the PRP fraction but undetectable in the PIP fraction. In contrast, the PMA2 homolog and OsRad21-3 were dominant in the PIP fraction and appeared undetectable in the PRP fraction (Fig. 3). The rice homolog of the maize xylanase has been identified in the coat-associated protein fraction (see Section 3.3). A blast search of the NCBI database revealed that rice genome contains a homolog (CAD29296) of *Nicotiana plumbaginifolia* PMA2. Together, these data indicate that this procedure efficiently enriches PRPs with or without only a few contaminants from PIPs.

Originally, each of the PRPs and PIPs was subjected to 2-DE with pH 3–10 gel strips, and the separation showed that most of the PRPs or PIPs were distributed around pH 4 to 7 (Suppl. Fig. 1A and B); therefore, the pH range strips of 4–7 were further used for the better solution of PRPs and PIPs in

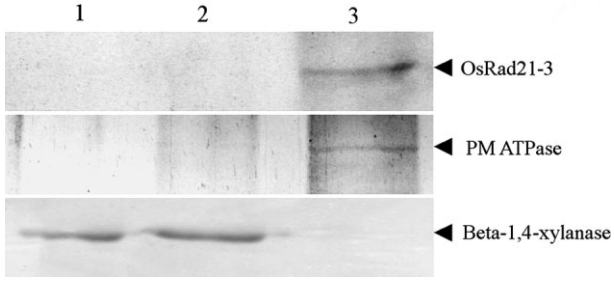

Figure 3. Western blot patterns of marker proteins detected with 1-D SDS-PAGE-separated pollen coat-associated proteins (1), PRPs (2) and PIPs (3) (see Section 2). These proteins were separated on 1-D SDS-PAGE with 12.5% SDS polyacrylamide gels and then transfered to PVDF membranes. The membranes were detected with rabbit polyclonal antibody against OsRad21-3 protein (1:2000 dilution, this antibody was prepared in our lab), a nucleus-loculizing protein [18], maize pollen coat beta-1,4-xylanase (1:200 dilution) (AAF70549) [15] whose rice homolog was identified in this study (NP_920933) and shared 70% amino acid identity with each other or plasma membrane H^+-ATPase PMA2 from *Nicotiana plumbaginifolia* (1:2000 dilution) (A43637) [17], which has a homolog (CAD29296) in rice genome with 90% amino acid identity to each other.

2-DE. Each separation was repeated at least 3 times to ensure reproducibility of protein patterns, and the representative gel patterns of the PRPs and PIPs are shown in Figs. 4 and 5.

The second separation did not increase the PRP spots, with 475 ± 8 spots (Fig. 4) as compared with 556 ± 12 spots (Suppl. Fig. 1A) resolved by the first separation. However, the second separation resolved more PIP protein spots (996 ± 27) (Fig. 5) than the first separation (631 ± 18 spots) (Suppl. Fig. 1B). Furthermore, 2-DE patterns of PRPs and PIPs showed characteristic differences (Figs. 4 and 5, and Suppl. Figs. 1A and B). Thus, PRPs were efficiently separated from the PIPs, and the PRP fraction contained a limited set of

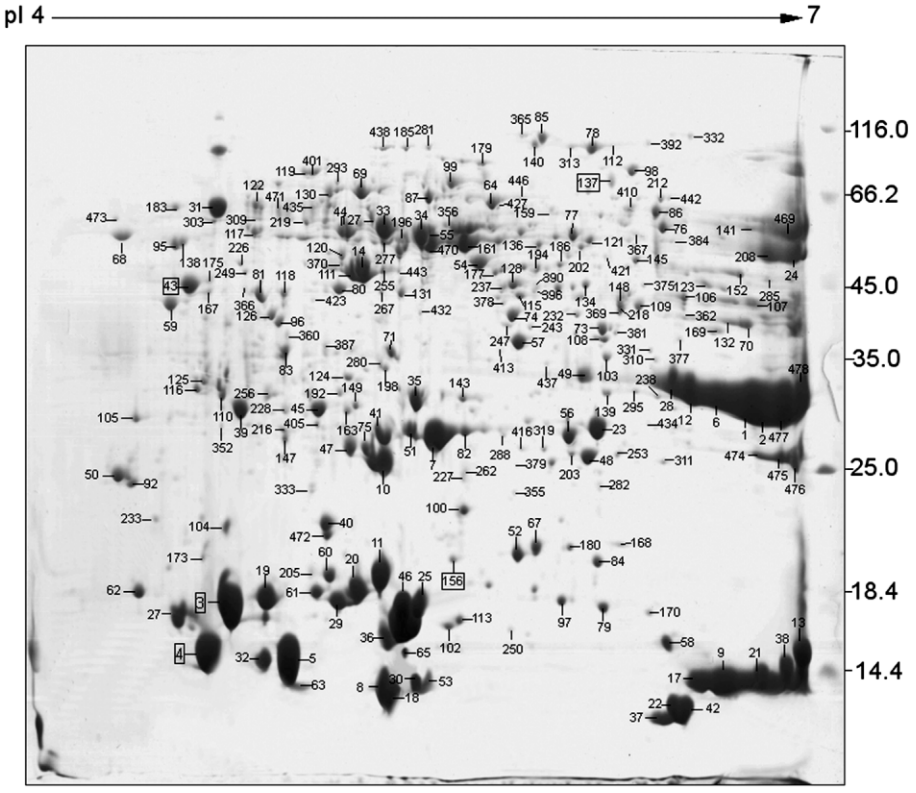

Figure 4. A representative 2-DE gel pattern of the prepared PRPs. The pH range used for IEF is 4 to 7 as indicated on top of the gel. SDS-PAGE was run in a 12.5% ExcelGel SDS gel (Amersham Biotech), and proteins were visualized by CBB staining. Numbers on the right indicate MM markers in kilodaltons. Of the detected 480 spots, 240 spots were identified by MALDI TOF MS and NanoESI Q-TOF MS/MS and therefore marked on the map. Five of them (marked by rectangle) represented *de novo*-sequenced proteins.

proteins, consistent with the Western blot analysis of the purity of each fraction (Fig. 3). All the visualized spots from PRP and PIP gels were analysed using ImageMaster 2D 2002.01 software, and listed according to each relative abundance, supplemented by the corresponding MM and p*I* data.

These protein spots were then subjected to MALDI-TOF MS (Fig. 6A) according to their relative abundance, and the identities of the spots are shown in Suppl. Table 1. To ensure the accuracy of protein identification, MALDI-TOF MS was internally calibrated with the masses of 2 trypsin autolysis products at m/z = 906.51 and m/z = 2273.16 to reach a typical mass measurement accuracy of 100 ppm, and MS-stringent criteria were followed for each spot digestion. The identified proteins must rank at the top hit with more than 4 matched peptides and the sequence coverage (SC) of more than 10%. Among the 486 identities listed in Suppl. Table 1, 477 (98.1%) had a SC of greater than 15%. The other 9 (1.9%) with a SC of lower than 15% but greater than 10%, were all matched with more than 5 peptides.

Some of the PRP spots that initially could not be identified by PMF searching according to our criteria were analyzed further by MS/MS (Fig. 6B and C). ESI Q-TOF MS/MS was internally calibrated with GLU1-Fibrinopeptide B (Sigma) to reach a typical mass measurement accuracy of 50 ppm. An identity was accepted only when its hit ranked as the top one with more than 2 peptide sequences matched. According to these criteria, 16 identities were obtained, with the exception of the identity representing protein NP_915642, which was identified by a single peptide match. Therefore, its MS/MS fragment ion pattern was verified by further inspection (Suppl. Table 2). Moreover, 5 of these analysed protein spots, not identified by searching MS/MS fragment ion patterns against databases, were sequenced *de novo* using Peptide Sequence Software (Table 1). The MS/MS data were processed *via* the Peptide Sequencing Program with strict criteria. MM tolerance and mass type were assumed to be 0.3 Da and monoisotopic, while the threshold value of peak and fragment ion tolerance were chosen as 0.15% and 0.15 Da, respectively. And most importantly, nearly complete y-ion series and partial complementary b-ion series needed to be present and the y-ions should correspond to peaks with high relatively intensity for this inspection.

On the basis of these analyses, we obtained 507 identities (from 507 unredundant spots). These identities represented 307 unique proteins (Table 2), 205 of which were from the PRP fraction (290 identities) and 149 from the PIP fraction (217 identities), with 47 overlapping between the 2 fractions.

Of the 158, only PRP fraction-derived unique proteins (Table 2), such as beta-1,4-xylanase, expansins, profilin, pectin methylesterase inhibitor, esterases, amylases, polygalacturonase, pollen allergens, cyclophilin and calreticulin were recognized as pollen coat/wall-associated or pollen-released proteins in maize and other species [15, 19, 20]. Proteins such as pectin methylesterase, pectin acetylesterase, beta-glucosidase, beta-glactosidase, subtilisin-like serine protease, peroxidases, apospory-associated protein, thiore

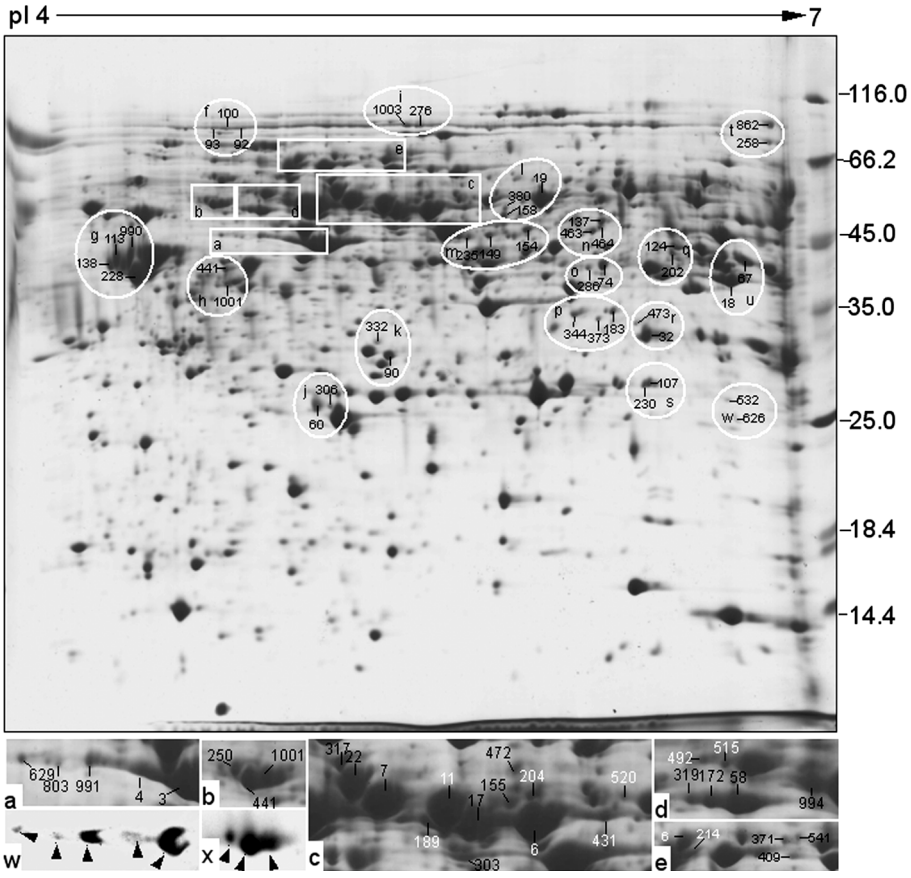

Figure 5. A representative 2-DE gel pattern of the prepared pollen interior proteins (PIPs). The illustration is identical to that described in Fig. 4. Isoforms of the partially identified proteins were marked directly on this map or in its enlarged part to show the shift in MM or/and p*I*.

a, actin AAO38821 isoforms (spots 4, 3, 629, 803, 991) confirmed by Western blotting with a antibody against actin (Sigma Corp, 1:3000 dilution) (w); b, beta-tubulin BAC82430 isoforms (spots 250, 441, 1001) confirmed by Western blotting with the antibody to tubulin (Sigma Corp, 1:10000 dilution) (x); c, UDP-glucose pyrophosphorylase AAF62555 (11, 189, 204 and 520) and vacuolar acid invertase AAF87246 (7, 17, 22, 155, 317 and 472); d, putative H^+-transporting ATP synthase NP_916591 (492 and 515) and ATP synthase beta chain Q01859 (58,172, 319 and 994); e, dnaK-type molecular chaperone BiP T03581 (61 and 214) and putative vacuolar proton-ATPase A subunit BAD27610 (371, 409 and 541); f, vacuolar proton-ATPase BAD45853 (92, 93 and 100); g, vacuolar acid invertase AAF87245 (113,138, 228 and 990); h, beta-tubulin BAC82430 (441 and 1001); i, putative isoamylase-type starch debranching enzyme XP_450961(276 and 1003); j, UMP/CMP kinase A XP_479205 (60 and 306); k, expressed protein related to glutamine amidotransferase class II AAT76419 (90 and 332); l, putative Myo-inositol-1-phosphate synthase NP_921086 (19, 158 and 380); m, putative mitochondrial ATP synthase beta chain NP_916979 (149,154 and 235); n, putative adenosylmethionine-8-amino-7-oxononanoate aminotransferase AAQ14479 (137, 463 and 464); o, reversibly glycosylated polypeptide CAA77235 (74 and 286); p, putative NADPH-thioredoxin reductase XP_467446 (183, 373 and 344); q, putative aldehyde dehydrogenase XP_475772 (124 and 202); r, peroxidase 78 precursor CAH69320 (32 and 473); s, superoxide dismutase[Mn] AAA62657 (107 and 230); t, putative subtilisin-like proteinase BAD35473 (258 and 862); u, putative glyceraldehydes 3-phosphate dehydrogenase CAD79700 (18 and 67); v, voltage-dependent anion channel XP_450604 (532 and 626).

doxin, esterase, and cellulose synthase, have previously been reported to be present in the extracellular matrix of somatic cells of other plant species [21], which indicates that the procedure used in this study can enrich and collect most pollen coat/wall-associated and pollen-released proteins, most of which were of high abundance in PRP gels (Fig. 4) and bore a signal peptide (Table 2). But an unexpected result was that some proteins related to signal transduction, carbon and energy metabolism *etc*. were also identified in the PRP fraction (Table 2). Probably, they leaked from the pollen cytoplasm because some eluted intact pollen grains with ruptured apertures, and some high-electron-dense substances containing microchannels and/or columellae were observed under SEM (Fig. 1H) and TEM (Fig. 1I). However, our Western blot results of evaluating the purity of PRPs (Fig. 3), combined with the data of recent wall proteomic studies of somatic cells [22, 23], preferred the possibility that at least some of them are extracellular or easily released proteins of the pollen. Further experiments to confirm the exact information on the localization of these proteins is a critical step

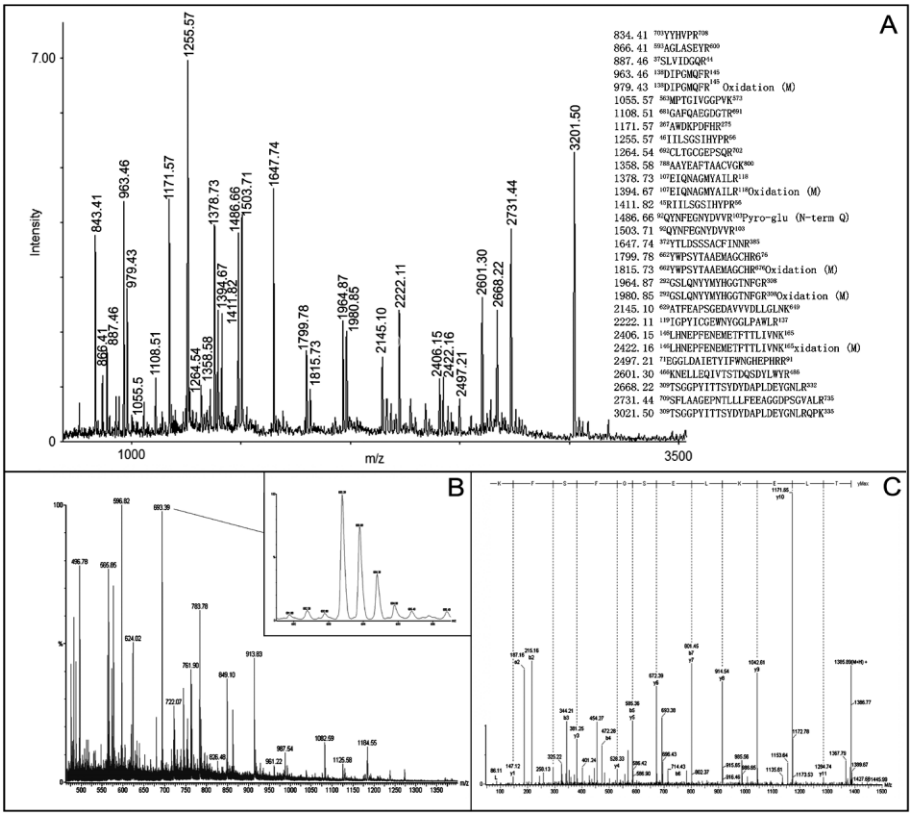

Figure 6. Representative MS spectra of proteins identified by MALDI TOF MS (A) and nano-ESI Q-TOF MS/MS (B and C).
A, PFM pattern of spot $R_4$85 marked in Fig. 4. The PMF generated by MALDI TOF MS (Materials and methods) was matched to the putative beta-galactosidase (NP_918096), by searching against the NCBI protein database with use of the search engine Matrix science, with 30 mass values matched among the searched 38 mass values and a sequence coverage of 39%. The matched peptides and their corresponding peaks were listed in the map. B, The MS pattern of the peptides from spot $R_4$156 marked in Fig. 4. Eight peaks of the peptide with double charge observed on the spectrum (marked by asterisk) were further subjected to MS/MS, and the inlet shows one of these peaks with double charge (m/z 693.39); C. the fragmentation doubly charged ion *m/z* 693.39 underwent *de novo* sequencing.

Table 1. The novel proteins identified by *de novo sequencing* with nanoESI Q-TOF MS/MS

Novel protein termed by us	Protein number on PRP gel (p*I* range 4–7)	Experimental		Peptide sequence by *de novo*	
		MM(Da)	p*I*	*m/z*	Peptide sequence
DnSP1	$R_4$4	14 145	4.69	688.43	NSTLNNDLMLLK
DnSP2	$R_4$43	51 816	4.07	483.61	LLALHASLTQLLR
				523.74	NFPSNLVAGK
DnSP3	$R_4$156	19 619	5.63	475.79	LLTSTSSGGK
				487.30	VTDSVLDPK
				496.80	WGQLYLGR
				596.81	VVYAYTVYSK
				693.39	TLEKLESGFSFK
DnSP4	$R_4$137	74 814	6.24	563.33	PKENQAVALR
				679.43	VLLDLKPKEFR
				744.92	NPAVLANSRVYER
DnSP5	$R_4$3	16 880	4.76	555.71	EYNVDTNQK
				571.71	FFFADQIVR
				636.24	AVDGSFVYNDGK
				760.35	RYVLSGLLSVDGLK

to understand their function. The challenge of the experiments lies mainly in the solubilization of extracellular or easily released proteins without contaminants, because of the thinner and microchannel-rich wall of mature rice pollen (Fig. 1D) and highly dynamic features of pollen plasma membrane and proteins [1].

3.3 Identification of 1-DE bands from the coat protein-enriched fraction by LC ESI Q-TOF MS/MS

The pollen coat, the outermost stratum of pollen surface, is essential to initial sexual contact and thus successful fertilization. To understand its function, we prepared a pollen coat

Table 2. The pollen proteins identified by 2-DE coupled with MALDI-TOF MS and nano-ESI Q-TOF MS/MS, and 1-D SDS-PAGE with nano-LC-Q-TOF MS/MS

Pr. No	Matched protein	Accession No.	MM (Da)	p*I*	SP[a)]	IN[b)]	Spots (bands) number of proteins from gels identified by MS		
							MALDI TOF MS[c)]	Nano-ESI Q-TOF MS/MS	$_{\mu}$LC Q-TOF MS/MS
	Signal transduction (33)								
1.	Putative Rho GDP dissociation inhibitor	NP_914805	24 817	4.52	–	–	$R_4$105, $R_3$523		
2.	Putative Rab GDP dissociation inhibitor	BAC79568	49 403	5.86	–	–	$R_4$378, $R_3$204		
3.	Rab GDP dissociation inhibitor, OsGDI1	AAB69870	49 670	5.96	–	–	–	–	C4
4.	Putative GTP-binding protein	BAD03576	44 305	6.30	–	–	$R_4$381, $R_3$306		
5.	Putative GTP-binding protein	NP_917635	24 987	6.38	–	–	$R_3$362		
6.	Putative GTP-binding protein	AAO60011	63 649	10.1	–	–	$I_4$291, $I_3$123		
7.	GTP-Binding protein beta subunit-like protein	NP_916988	36 665	5.97	–	–	$R_4$108		
8.	Putative calreticulin precursor	AAP46258	50 078	4.67	S	3	$R_4$175, $R_4$183, $R_4$303, $R_3$108, $R_3$115		C2, C3
9.	Putative calreticulin precursor	XP_477251	48 450	4.47	S	2	$R_4$68, $R_4$473		
10.	C2 domain protein-like	BAC79554	18 224	5.17	–	2	$R_4$19, $R_4$61, $R_3$543		C11
11.	Zinc finger and C2 domain protein-like	XP_478258	18 899	5.71	–	–	$R_4$52		
12.	Putative elicitor-responsive gene-3 (a C2 domain- containing protein)	XP_466973	15 766	4.56	–	–	$R_4$62		
13.	Putative Avr9/cf-9 rapidly elicited protein (a calmodulin-like protein)	BAC66766	20 631	4.51	–	–	$R_4$173, $R_3$276		
14.	Putative SnRK1b protein kinase	BAC83176	59 920	6.80	S	–	$I_4$242, $I_3$129		
15.	Putative serine/threonine protein kinase 2, CIPK2	BAA92972	51 933	9.28	–	–	$I_4$262, $I_3$151		
16.	MAP kinase 6 (Serine/Threonine protein kinases)	BAD69291	45 172	5.45	–	–	$I_4$94		
17.	Putative serine/threonine protein kinase	BAD33903	39 978	5.91	–	–	$I_4$446		
18.	Serine/Threonine protein kinase-like	NP_908580	89 501	6.86	–	–	$I_4$992		
19.	Putative TGF-beta receptor-interacting protein (WD40)	XP_481483	36 527	5.94	–	–	$I_4$455		
20.	Putative WD-40 repeat protein, similar to serine/threonine receptor-associated protein NP_035629 of *M. musuculus*	BAD32940	38 081	5.43	–	–	$I_4$283		
21.	Putative 14-3-3 protein	AAK38492	29 160	4.81	–	–	$R_4$125, $I_4$238, $R_3$325, $I_3$152		C7, C8
22.	Predicted OJ1124_B05.7 gene product; containing Smart 00101 14-3-3 domain, putative 14-3-3 protein	XP_507235	28 979	4.78	–	–	$R_4$116		
23.	GF14-d protein	T04154	29 244	4.83	–	–	$R_4$352, $R_3$110		C7, C8
24.	GF14-c protein	T04153	28 808	4.82	–	–	–	–	C8
25.	Phosphatase 2A regulatory A subunit	CAB51803	65 658	4.90	S	–	$R_4$219, $I_4$213, $I_3$215		
26.	Putative altered response to gravity 1 protein (ARG1)	NP_918662	44 915	5.93	–	–	$R_4$432, $R_3$281		
27.	Putative CC-NBS-LRR resistance protein	BAC84194	103 888	5.24	–	–	$R_3$244		
28.	Cyclophilin 1	S48018	19 186	7.67	–	–	$R_3$326		
29.	Cyclophilin 2	AAA57046	18 319	8.61	–	2	$R_3$109, $R_3$151		C10
30.	Unknown protein; similar to *Arabidopsis peptidyl-prolyl cis-trans isomerase (P34791)*	AAG03106	19 260	8.87	S	–	$R_3$298		
31.	Putative soluble inorganic pyrophosphatase	AAK98675	22 541	5.71	–	(4)	$R_4$82, $I_4$85, $I_4$261, $I_4$288, $I_4$294, $I_3$5, $I_3$36		
32.	Putative soluble inorganic pyrophosphatase	XP_475313	25 568	5.43	–	–	$I_4$797		
33.	P0505D12.23; putative inorganic pyrophosphatase	NP_915642	23 242	5.59	–	–	–	$R_4$56	

Table 2. Continued

Pr. No	Matched protein	Accession No.	MM (Da)	p*I*	SP[a)]	IN[b)]	Spots (bands) number of proteins from gels identified by MS		
							MALDI TOF MS[c)]	Nano-ESI Q-TOF MS/MS	$_{\mu}$LC Q-TOF MS/MS
	Vesicle trafficking (7)								
34.	OSJNBa0033G05.19; containing Coatomer E domain pfam04737, putative Coatomer epsilon subunit	XP_474096	32 340	5.74	–	–	$I_4$997		
35.	Putative alpha-soluble NSF attachment protein	XP_481268	32 750	5.04	–	–	$I_4$169		
36.	Putative annexin	BAD37678	35 984	6.21	–	–	$I_4$299		
37.	Endosperm lumenal binding protein	AAB63469	73 666	5.30	S	–	$I_4$194		
38.	Putative lysophospholipase 2	NP_916484	27 254	6.44	–	–	$R_4$180		
39.	Unkown protein; containing TRAP_beta domain pfam05357, translocon-associated protein beta (TRAPB) family protein	BAB62640	20 191	9.89	S	–	–	–	C10
40.	Unknown protein; containing Tim17 domain pfam02466, mitochondrial import inner membrane translocase Tim17/Tim22/Tim23 family protein	AAN59775	19 236	8.33	–	–	–	–	C10
	Transcriptional regulation-related (8)								
41.	Putative leucine-rich protein	XP_466501	55 345	5.51	–	–	$I_4$208		
42.	MCT-1 protein-like (containing RNA-binding domain pfam01472, probable modifier of RNA)	NP_908610	20 333	7.75	–	–	$R_3$542		
43.	Putative centromere/microtubule binding protein (containing RNA-binding domain pfam01472, probable modifier of RNA)	BAC16386	65 826	9.16	–	–	$R_4$228, $R_3$199		
44.	Putative MAR-binding protein MFP1	NP_914440	87 338	5.10	–	–	$I_3$162		
45.	B1129G05.10; CCCH type Zinc finger-containing protein	XP_463338	77 523	5.65	–	–	$I_4$62		
46.	OSJNBa0086A10.7; RING-H2 Zinc finger domain containing protein	NP_918125	29 460	6.74	–	–	$R_4$139		
47.	Putative arsenite inducible RNA associated protein (containing AN1-type Zinc finger and C2H2 type Zinc finger	BAC79697	31 872	8.61	–	–	$R_3$142		
48.	Unknown protein; Myb_DNA-binding domain pfam00249-containing protein	AAV44074	31 680	6.61	–	–	$I_4$156		
	Transposition (2)								
49.	Hypothetical protein; containing transposase 28 domain pfam04195, transposase 28 family	XP_468942	45 139	9.18	–	–	$I_4$800		
50.	OSJNBb0032E06.9; containing integrase core domain pfam00665 and reverse transcriptase domain pfam00078	CAE02251	138 142	8.96	–	–	$R_3$77		
	Cytoskeleton dynamics (11)								
51.	Actin	AAO38821	41 786	5.30	–	2 (5)	$R_4$360, $R_4$387, $I_4$3, $I_4$4, $I_4$629, $I_4$803, $I_4$991, $R_3$57, $I_3$4, $I_3$18, $I_3$22, $I_3$38, $I_3$64, $I_3$112, $I_3$127	$R_4$111	
52.	Alpha-tubulin	AAG16905	49 787	4.88	–	–	$R_4$366, $I_4$170, $R_3$350, $I_3$126		
53.	Alpha-tubulin	P28752	49 622	4.92	–	–	$R_4$423, $R_3$146		

Table 2. Continued

Pr. No	Matched protein	Accession No.	MM (Da)	p*I*	SP[a)]	IN[b)]	Spots (bands) number of proteins from gels identified by MS		
							MALDI TOF MS[c)]	Nano-ESI Q-TOF MS/MS	$_{\mu}$LC Q-TOF MS/MS
54.	Beta-tubulin	BAC82430	49 602	4.77	–	2 (2)	$R_4$117, $R_4$118, $I_4$250, $I_4$441, $I_4$1001, $I_3$42, $R_3$75		
55.	Beta-tubulin	NP_912596	50 253	4.73	–	–	$R_4$167, $R_3$76		
56.	Profilin A	NP_920667	14 234	4.91	–	2	$R_4$102, $R_4$113, $R_3$37, $R_3$40		
57.	Putative 66 kDa stress protein-similar to *Arabidopsis* actin interacting protein 1(AIP1)	NP_909076	67 097	6.48	–	2	$R_4$384, $R_4$410, $R_3$113		
58.	Putative actin-depolymerizing factor 2	BAC16183	16 052	5.52	–	–	$R_4$11, $I_4$205, $I_3$139		C11
59.	Putative actin depolymerizing factor	NP_922379	17 548	5.94	S	–	$R_4$238		
60.	Putative actin-depolymerizing factor	BAD27692	16 211	5.56	–	–	–	$R_4$20	
61.	OSJNBb0012E24.5; containing actin depolymerisation factor/cofilin domain CD00013	CAE01864	15 874	5.55	–	–	$R_4$29		
	Protein synthesis, assembly and degradation (45)								
62.	Translational elongation factor Tu	AAL55261	48 393	6.04	–	–	$R_4$128, $I_4$996, $I_3$143		
63.	Translational elongation factor 1A	BAB17334	89 585	8.63	–	–	$I_4$398, $I_3$113		
64.	Translational elongation factor 1A	BAA23657	49 347	9.19	–	–	$R_3$7		
65.	Elongation factor 1 beta	XP_479153	24 904	4.36	–	–	$I_4$148		
66.	Putative elongation factor 2	XP_465992	94 987	5.85	–	–	$I_4$923		
67.	Putative 60S ribosomal protein	BAD03800	34 251	10.70	–	–	$R_3$217		
68.	30S ribosomal protein S18	BAC24844	17 652	11.00	–	–	–	–	C11
69.	40S ribosomal protein S16	P46294	16 877	10.9	–	–	–	–	C11
70.	Eukaryotic initiation factor 4A	P35683	46 902	5.29	–	2	$R_4$255, $R_4$443, $R_3$168, $R_3$170		
71.	Putative translational inhibitor protein (probable inhibitor of translational initiation)	BAC20708	18 806	9.65	–	–	–	–	C10
72.	Translationally controlled tumor protein homolog	P35681	18 934	4.51	–	4	$R_4$104, $R_4$233, $R_3$220, $R_3$262	$R_4$50, $R_4$92	
73.	Heat shock protein 82	P33126	80 144	5.10	–	–	–	–	C1
74.	Heat shock protein cognate 70	AAO65876	71 267	5.10	–	–	$R_4$130, $R_3$121		
75.	Heat shock protein 70	CAA47948	70 953	5.17	–	–	$R_4$309, $R_3$370		
76.	Putative heat shock 70 kD protein, mitochondrial precursor	AAO17017	70 403	5.46	–	–	$I_4$197, $I_3$135		
77.	Putative 60 kD chaperonin beta subunit	BAA92724	64 046	5.60	–	–	$I_4$216, $I_3$104		
78.	Mitochondrial chaperonin 60	AAN05528	60 812	5.71	–	–	$I_4$181, $I_3$49	$R_4$127	
79.	dnaK-type molecular chaperone BiP	T03581	73 495	5.30	S	3 (2)	$R_4$119, $R_4$293, $R_4$401, $I_4$214, $I_4$61, $R_3$91, $R_3$171, $R_3$437, $I_3$90, $I_3$62		
80.	Putative disulfide isomerase	AAS55771	38 179	6.30	S	–	$R_4$106		
81.	Protein disulfide isomerase	BAA92322	33 496	4.81	S	2	$R_4$122, $R_4$31		
82.	Putative disulfide-isomerase precursor	NP_910169	39 888	6.58	S	–	$R_4$377, $R_3$103		
83.	Putative protein disulfide isomerase	NP_908816	41 114	6.43	S	3	$R_4$218, $R_4$148, $R_4$369, $R_3$135, $R_3$428, $R_3$467		
84.	Putative prohibitin	BAC84245	31 935	9.77	S	–	$I_3$145		
85.	Putative prohibitin	BAC07170	38 981	10.03	S	–	–	–	C8
86.	Putative mitochondrial processing peptidase alpha chain precursor	NP_914556	90 235	8.57	–	2	$R_4$208, $R_4$152, $I_4$64, $R_3$290, $R_3$297, $I_3$3		

Table 2. Continued

Pr. No	Matched protein	Accession No.	MM (Da)	p*I*	SP[a]	IN[b]	Spots (bands) number of proteins from gels identified by MS		
							MALDI TOF MS[c]	Nano-ESI Q-TOF MS/MS	$_{\mu}$LC Q-TOF MS/MS
87.	Putative mitochondrial processing peptidase alpha subunit precursor	BAB55500	47 465	7.64	–	–	$I_4$151, $I_3$31		
88.	Putative mitochondrial processing peptidase	BAD72225	54 141	6.65	–	–	$I_4$31		
89.	20S proteasome subunit alpha 1	Q9LSU3	27 556	6.19	–	–	$R_4$311, $I_4$134, $R_3$423, $I_3$186		
90.	20S proteasome subunit alpha 2	Q9LSU2	25 828	5.39	–	–	$I_4$594, $I_3$133		
91.	20S proteasome subunit alpha 6	P52428	29 897	5.37	–	(2)	$I_4$220, $I_4$563		
92.	20S proteasome subunit alpha 7	NP_915931	27 221	5.75	–	–	$I_4$341, $I_3$148		
93.	20S proteasome subunit beta 1	BAA96834	26 257	5.47	–	–	$I_4$338, $I_3$167		
94.	20S proteasome subunit beta 2	BAA96835	28 979	6.45	–	–	$I_4$188, $I_3$118		
95.	20S proteasome subunit beta 5	BAA96838	29 865	5.73	–	–	$I_4$301, $I_3$146		
96.	Putative 26S proteasome regulatory particle triple-A ATPase subunit 5a	BAD72286	47 978	4.94	–	–	$I_4$433		
97.	Putative ubiquitin-specific protease 3	NP_912571	42 685	5.80	–	–	$R_4$97		
98.	Ubiquitin-conjugating enzyme OsUBC5b	XP_464900	16 606	7.71	–	–	$R_3$149		
99.	Putative UFD1	BAB89159	62 797	6.22	–	–	$I_4$63, $I_3$55		
100.	P0492F05.26; containing AAA^+ domain pfam0004, putative ATPases of the AAA^+ class	NP_913449	90 012	7.19	–	–	$I_4$241		
101.	Ulp1 protease-like protein	BAD36141	92 460	4.93	–	–	$R_4$42		
102.	Peptidase S28 family, putative serine carboxypeptidase	AAG13567	56 087	8.70	S	–	$I_4$154, $I_3$217		
103.	Predicted OJ1148_D05.1 gene product; peptidase M20 family, putative glutamate carboxypeptidase	XP_506898	48 989	5.19	–	–	$I_4$49		
104.	OSJNBa0065O17.12; Peptidase S8 family, highly similar to subtilisin-like serine protease	XP_473475	84 143	7.57	S	–	$R_3$141		
105.	Peptidase S8 family, putative subtilisin-like proteinase	BAD35473	84 117	6.61	S	(2)	$I_4$862, $I_4$258		
106.	Aspartic proteinase oryzasin 1 precursor	AAU10663	54 723	5.20	S	–	$R_4$110		
	Stress responses (14)								
107.	Unnamed protein product; containing AHP domain COG0678, putative peroxiredoxin	NP_912904	20 861	7.77	–	–	$R_4$168, $R_3$160		
108.	L-Ascorbate peroxidase	BAB17666	27 101	5.21	–	3	$R_4$149, $R_4$47, $R_4$45, $I_4$104, $R_3$23		C9
109.	L-Ascorbate peroxidase	T03595	27 139	5.42	–	6	$R_4$227, $R_4$262, $R_4$379, $R_4$416, $R_4$41, $R_4$7, $R_3$19, $R_3$250		C9
110.	Putative monodehydroascorbate reductase	BAC98552	52 726	6.84	–	2	$R_4$24, $R_4$121 $R_3$112		
111.	Superoxide dismutase [Cu-Zn]	AAA33917	15 224	5.71	S	–	$R_4$250, $R_3$119		
112.	Superoxide dismutase [Mn]	AAA62657	24 982	6.5	S	(2)	$I_4$107, $I_4$230	$R_4$319	
113.	Glutathione S-transferase	T02765	25 603	6.25	–	–	$R_4$282, $R_3$210		
114.	Glutathione S-transferase II	NP_916246	24 303	5.77	–	–	$R_4$23		
115.	Probable glutathione-disulfide reductase	T03766	53 929	6.24	–	–	$I_4$102		
116.	GSH-dependent dehydroascorbate reductase 1	BAA90672	23 712	5.65	–	–	$R_4$48		
117.	Selenium-binding protein-like	XP_550496	46 933	6.37	–	–	$R_4$86		
118.	Putative legumin	AAV44198	38 456	5.81	–	–	$R_4$57, $I_4$150		
119.	Putative legumin-like protein	NP_914389	40 581	5.64	–	–	$I_4$436		

Table 2. Continued

Pr. No	Matched protein	Accession No.	MM (Da)	p*I*	SP[a)]	IN[b)]	Spots (bands) number of proteins from gels identified by MS		
							MALDI TOF MS[c)]	Nano-ESI Q-TOF MS/MS	$_{\mu}$LC Q-TOF MS/MS
120.	OSJNBa0084K11.5 protein; containing TRX-A domain COG0526, putative thio-disulfide isomerase/thioredoxin	CAE01844	14 768	5.53	–	–	$R_4$79		
	Wall remodeling and metabolism (35)								
121.	Glycosyl hydrolase family 10, putative 1,4-beta-xylanase	NP_920933	59 708	8.79	S	2	$R_3$267, $R_3$397		C8
122.	Unnamed protein product; containing glycosyl hydrolase 3 N terminal domain pfam 00933 and C terminal domain pfam01915; glycosyl hydrolase family 3, putative beta glucanase	AAL58963	92 850	8.43	S	–	–	–	C1, C2
123.	Glycosyl hydrolase family 28, putative polygalacturonases	BAD03446	43 463	8.84	S	–	$R_3$329		
124.	Glycosyl hydrolase family 28, putative exopolygalacturonase precursor	XP_464471	44 519	7.47	S	–	$R_3$154		
125.	Glycosyl hydrolase family 17, putative glucan endo-1,3-beta-D-glucosidase	BAD33320	36 487	6.29	S	–	$R_4$203		
126.	Glycosyl hydrolase family 35, putative beta-galactosidase	NP_920740	91 480	6.01	S	2	$R_4$112, $R_4$392, $R_3$84, $R_3$164		
127.	Glycosyl hydrolase family 35, putative beta-galactosidase	NP_918096	92 850	5.76	S	4	$R_4$85, $R_4$98, $R_4$313, $R_4$365		C1
128.	Putative pectin methylesterase	BAC83510	61 657	5.50	S	–	$R_4$123, $R_3$349		
129.	Unnamed protein product; containing PMEI domain pfam04043, putative pectin methylesterase inhibitor	NP_912762	18 999	5.93	S	–	$R_4$25, $R_3$11		
130.	OSJNBa0041A02.14; containing PAE domain pfam03283, putative pectin acetylesterase	CAD41867	42 948	8.10	S	–	$R_3$372		
131.	Putative esterase D	BAB90254	35 810	8.38	–	–	$R_3$418		
132.	Putative cellulase	XP_468087	54 962	8.02	S	–	$R_3$202		
133.	Putative beta-expansin	AAN60491	28 608	6.34	S	9	$R_4$1, $R_4$2, $R_4$6, $R_4$49, $R_4$100, $R_4$253, $R_4$474, $R_4$477, $R_4$478, $R_3$45, $R_3$180, $R_3$191		C7
134.	Putative beta-expansin	NP_912531	29 489	6.88	S	2	$R_4$475, $R_4$476		
135.	Beta-expansin OsEXPB13	AAL24476	29 228	8.01	S	–	$R_4$12		C9
136.	Putative beta-expansin	NP_912530	24 653	5.55	S	–	$I_4$135		
137.	Major pollen allergen Ory s 1 precursor	Q40638	28 479	8.53	S	2	$R_4$13, $R_4$38, $R_3$181, $R_3$266		C8
138.	Putative pollen specific protein C13 precursor	BAD54680	17 488	5.15	S	2	$R_4$40, $R_4$472		
139.	OSJNBa0050F15.10; putative pollen allergen 1	XP_471811	12 380	7.82	S	–	$R_4$22		
140.	Putative group 3 pollen allergen	BAD37571	12 364	5.37	S	5	$R_4$8, $R_4$18, $R_4$30, $R_4$37, $R_4$53		C14
141.	Putative group 3 pollen allergen	BAD45861	12 296	6.29	S	3	$R_4$36, $R_4$46, $R_4$65		
142.	OSJNBa0050F15.8, putative pollen allergen	CAD40508	12 311	5.46	S	2	$R_4$5, $R_4$63, $R_3$367		C13, C14
143.	Putative peroxidase (class III peroxidase 31 precursor)	XP_467718	47 858	5.84	S	(3)	$R_4$54, $I_4$391, $I_4$303, $I_4$83		
144.	Class III peroxidase 36 precursor	CAH69278	51 182	4.85	S	(2)	$R_4$59, $I_4$1, $I_4$460		
145.	Class III peroxidase 78 precursor	CAH69320	35 865	6.25	S	(2)	$I_4$473, $I_4$32		

Table 2. Continued

Pr. No	Matched protein	Accession No.	MM (Da)	p*I*	SP[a)]	IN[b)]	Spots (bands) number of proteins from gels identified by MS		
							MALDI TOF MS[c)]	Nano-ESI Q-TOF MS/MS	$_{\mu}$LC Q-TOF MS/MS
146.	UDP-glucose pyrophosphorylase	AAF62555	51 638	5.46	–	4 (6)	$R_4$55, $R_4$196, $R_4$267, $R_4$470, $I_4$6, $I_4$11, $I_4$189, $I_4$204, $I_4$431, $I_4$520, $R_3$5, $R_3$17, $R_3$148, $R_3$382, $I_3$21, $I_3$33		C6
147.	UDP-glucuronic acid decarboxylase	BAB84334	39 284	7.16	–	–	$R_3$336		
148.	Putative GDP-mannose pyrosphorylase	BAD05471	39 601	6.52	S	–	$R_3$68		
149.	Putative Myo-inositol-1-phosphate synthase	NP_921086	55 980	6.00	–	(3)	$R_4$76, $I_4$19, $I_4$158, $I_4$380, $R_3$43, $I_3$8, $I_3$89		C3, C4
150.	Putative myo-inositol monophosphatase	AAT76319	29 297	5.44	–	–	$R_4$198, $I_4$203		
151.	Reversibly glycosylated polypeptide	CAA77235	41 322	5.82	–	3 (2)	$R_4$115, $R_4$390, $R_4$396, $I_4$74, $I_4$286, $R_3$184, $I_3$17, $I_3$54		
152.	Putative reversibly glycosylated polypeptide	XP_479089	41 652	6.01	–	–	$I_4$357		
153.	Cellulose synthase-like F7, OsCsLF7	DAA01754	90 083	9.31	–	–	$R_3$86		
154.	Putative dirigent-like protein	AAT77906	20 279	6.18	S	–	$R_4$67		
155.	Apospory-associated protein C-like	XP_450550	35 051	5.90	S	–	$R_4$83		
	Carbohydrate and energy metabolism (81)								
156.	Putative alpha-amylase precursor	XP_467955	47 855	5.07	S	2	$R_4$226, $R_4$249		
157.	Putative isoamylase-type starch debranching enzyme	XP_450961	79 952	5.40	–	(2)	$R_4$179, $I_4$276, $I_4$1003		
158.	alpha 1,4-glucan phosphorylase H isozyme	AAG45939	91 434	7.36	–	4 (3)	$R_4$185, $R_4$281, $R_4$332, $R_4$438, $I_4$377, $I_4$451, $I_4$993, $R_3$215, $R_3$292, $R_3$476, $R_3$53		
159.	alpha 1,4-glucan phosphorylase H isozyme	NP_915521	94 867	6.82	–	(2)	$I_4$999, $I_4$270		
160.	Vacuolar acid invertase	AAF87245	71 264	5.06	S	3 (4)	$R_4$120, $R_4$138, $I_4$113, $I_4$138, $I_4$228, $I_4$990, $R_3$99, $R_3$132, $R_3$153	$R_4$95	
161.	Vacuolar acid invertase	AAF87246	71 720	5.31	–	(6)	$I_4$7, $I_4$17, $I_4$22, $I_4$155, $I_4$317, $I_4$472, $I_3$95, $I_3$32, $I_3$92, $I_3$13, $I_3$23, $I_3$272		C1
162.	Hexokinase I	AAK51559	54 264	5.76	–	–	$R_4$177, $R_3$515		C6
163.	Putative fructokinase I	NP_915138	34 698	5.07	–	–	$R_4$126, $R_3$152		
164.	Putative fructokinase II	AAL26573	35 494	5.02	–	2	$R_4$96, $R_4$192, $R_3$162		
165.	Phosphoglucomutase	AAK18846	62 910	5.40	–	2	$R_4$99, $R_4$356, $R_3$54		
166.	beta-phosphoglucomutase-like protein	BAD36300	27 377	4.94	–	–	$R_4$39		
167.	Phosphoglucose isomerase A	P42862	62 488	6.80	–	–	$R_4$141, $R_3$120		
168.	Phosphoglucose isomerase A	NP_919066	62 484	6.80	–	–	$R_4$469, $I_4$118, $R_3$114, $I_3$70		
169.	Phosphoglucose isomerase B	P42863	62 380	6.45	–	–	$R_4$367, $R_3$56		
170.	Putative UDP-glucose dehydrogenase	AAT78767	51 987	6.53	–	–	$I_4$491		
171.	Putative sucrose-6F-phosphate phosphohydrolase	NP_918765	47 035	5.70	–	–	$R_4$136		
172.	Fructose-bisphosphate aldolase class-I, cytoplasmic isoenzyme	P17784	38 786	8.50	–	–	$I_3$175		
173.	Fructose-bisphosphate aldolase class-I, isoenzyme	S65073	38 799	8.40	–	–	$I_3$212		

Table 2. Continued

Pr. No	Matched protein	Accession No.	MM (Da)	p*I*	SP[a)]	IN[b)]	Spots (bands) number of proteins from gels identified by MS		
							MALDI TOF MS[c)]	Nano-ESI Q-TOF MS/MS	$_{\mu}$LC Q-TOF MS/MS
174.	Putative fructose-bisphosphate aldolase	AAT85154	39 238	6.96	–	–	$R_3$539		
175.	Putative triosephosphate isomerase	XP_462797	27 046	5.38	–	2	$R_4$51, $R_4$405, $I_4$82, $R_3$52		
176.	Putative phosphoglycerate mutase	BAD73342	60 980	5.42	–	–	$I_4$278		
177.	Cytosolic glyceraldehyde-3-phosphate dehydrogenase	AAN59792	23 366	7.88	–	3	$R_3$118, $R_3$140, $R_3$251		
178.	Cytosolic glyceraldehyde-3-phosphate dehydrogenase	Q42977	36 470	6.61	–	–	$R_4$1, $R_3$83		
179.	Putative glyceraldehyde-3-phosphate dehydrogenase	CAD79700	42 026	6.40	–	(2)	$R_4$28, $I_4$18, $I_4$67, $I_3$94, $R_3$229, $I_3$27		
180.	OJ000223_09.15; containing GapA domain COG0057, putative glyceraldehyde-3-phosphate dehydrogenase	CAE02009	36 750	6.34	–	3	$R_4$1, $R_4$70, $R_3$24, $R_3$95		
181.	Putative glyceraldehyde-3-phosphate dehydrogenase	XP_464291	43 461	8.99	–	–	$R_3$345		
182.	Putative glyceraldehyde-3-phosphate dehydrogenase	XP_506852	3 6716	7.68	–	–	$R_3$93		
183.	Enolase	AAP94211	47 942	5.41	–	2	$R_4$33, $R_4$277, $R_3$5, $R_3$12	$R_4$34, $R_4$161	
184.	Putative enolase	AAM74365	33 603	5.86	–	–	–	–	C12
185.	Enolase	Q42971	47 956	5.51	–	–	–	–	C4, C6
186.	Cytoplasmic aldolase	BAA02729	39 151	6.56	–	(3)	$R_4$285, $I_4$998, $R_3$411, $I_3$37, $I_3$85, $I_3$207		
187.	Unnamed protein product; containing pyruvate_kinase domain CD00288, putative pyruvate kinase	NP_912984	54 568	8.14	–	–	$R_3$247		
188.	Putative pyruvate kinase	NP_922817	61 834	6.01	–	–	$I_4$1000		
189.	Putative pyruvate dehydrogenase E1 alpha subunit	XP_467697	43 017	7.64	–	–	$I_4$65		
190.	Putative 2,3-bisphosphoglycerate-independent phosphoglycerate mutase	BAD82294	60 980	5.42	–	–	$R_4$87, $R_3$42	$R_4$69	
191.	Putative xylulose kinase	XP_479289	62 152	5.42	–	–	$I_4$277		
192.	Putative aconitate hydratase	XP_480473	98 591	5.67	–	–	$R_4$140, $I_4$191		
193.	Aconitase	CAA58046	101 439	5.98	–	–	–	$R_4$78	
194.	Putative phosphoglycerate kinase, cytosolic	XP_464267	42 196	5.64	–	–	$I_4$191		
195.	Putative cytosolic phosphoglycerate kinase 1	BAD45421	42 310	6.19	–	–	$I_4$27		
196.	Putative aldehyde dehydrogenase	XP_475772	56 764	8.66	–	(2)	$I_4$124, $I_4$202		
197.	Putative dehydrogenase precursor	XP_469854	40 438	6.73	–	–	$I_4$147		
198.	Predicted OJ1234_B11.18 gene product; contain COG0045 domain, putative succinyl-CoA synthetase, beta subunit	XP_506871	45 405	5.98	–	–	$R_4$80		
199.	Glyoxalase I	XP_480480	32 875	5.51	–	–	$I_4$649		
200.	Predicted OSJNBa0056O06.9-2 gene product; glyoxalase/bleomycin resistance protein/dioxygenase superfamily, highly similar to glyoxalase	XP_507569	32 875	5.51	–	–	$R_4$71		
201.	P0694A04.29; highly similar to aldose 1-epimerase	NP_917343	25 993	5.89	–	–	$R_4$84		
202.	Putative aldose reductase	NP_915489	33 513	5.85	–	–	$R_4$413, $R_3$200		
203.	Putative carbonic anhydrase	BAD33953	34 260	8.35	–	–	$I_4$12		
204.	Putative dihydrolipoamide acetyltransferase	NP_910215	71 720	5.31	–	–	$I_4$139, $I_3$71		

Table 2. Continued

Pr. No	Matched protein	Accession No.	MM (Da)	p*I*	SP[a)]	IN[b)]	Spots (bands) number of proteins from gels identified by MS		
							MALDI TOF MS[c)]	Nano-ESI Q-TOF MS/MS	$_{\mu}$LC Q-TOF MS/MS
205.	Putative dihydrolipoamide S-acetyltransferase	BAD06281	58 961	8.21	–	–	$I_4$407, $I_3$79		
206.	Unknown protein; containing COG0508, putative dihydrolipoamide acetyltransferase	BAC81178	58 735	8.65	–	–	$I_4$549, $I_3$108		
207.	OSJNBa0072K14.5; containing COG0508, putative dihydrolipoamide acetyltransferase	CAD40552	48 253	8.70	–	–	$I_4$160, $I_3$55		
208.	Putative dihydrolipoamide dehydrogenase precursor	NP_908725	52 610	7.21	S	–	$R_3$104		
209.	Putative dihydrolipoamide dehydrogenase	XP_475628	53 098	7.63	–	–	$I_4$273		
210.	Citrate synthase	AAG28777	52 195	7.71	–	2	$R_3$35, $R_3$190, $I_4$44, $I_3$157		
211.	Putative citrate synthetase	BAA82390	54 668	6.41	–	–	$I_3$29		
212.	Cytoplasmic malate dehydrogenase	BAA02729	35 888	5.75	–	–	$R_4$74		
213.	Putative malate dehydrogenase	NP_917241	35 439	8.74	–	–	$R_4$295, $R_3$29		
214.	NADP malic enzyme	AAQ99276	62 895	5.52	–	3	$R_4$64, $R_4$427, $R_4$446, $I_4$95, $R_3$49, $R_3$174, $R_3$214, $I_3$254		
215.	NADP-specific isocitrate dehydrogenase	AAD37810	46 114	6.29	–	–	$R_4$375, $R_3$324		
216.	NADP-specific isocitrate dehydrogenase	NP_917313	46 356	6.34	–	–	$R_4$109		
217.	Unnamed protein product, putative isocitrate dehydrogenase	NP_912978	39 417	7.10	–	–	$R_4$310, $I_4$115, $R_3$127, $I_3$35		
218.	OSJNBa0044K18.22; containing pfam00180 Iso_dh domain, putative isocitrate/ isopropylmalate dehydrogenase	CAE05880	36 540	5.77	–	2	$R_4$73, $R_4$134, $I_4$153, $I_3$19		
219.	Putative NADPH-thioredoxin reductase	XP_467446	34 940	6.19	–	(3)	$I_4$373, $I_4$183, $I_4$344		
220.	Putative succinate dehydrogenase flavoprotein alpha subunit	BAC83515	68 810	6.61	–	2	$R_4$212, $R_4$442, $R_3$494, $R_3$69		
221.	Aspartate transaminase precursor	JC5125	47 465	7.64	–	–	$R_4$107		
222.	Alcohol dehydrogenase 1	AAF34414	40 958	6.20	–	2	$R_4$169, $R_4$331, $R_3$111		
223.	Putative 6-phosphogluconolactonase	BAD33762	29 061	5.46	–	–	$I_4$80	$R_4$35	
224.	Putative 6-phosphogluconolactonase	XP_483640	34 680	7.77	–	–	$I_4$488		
225.	Putative cytochrome b5 reductase	NP_916477	32 146	9.11	–	–	$R_3$248		
226.	ATP synthase alpha chain, mitochondrial	P15998	55 247	5.85	–	(5)	$I_4$45, $I_4$309, $I_4$361, $I_4$382, $I_4$660, $I_3$7, $I_3$9, $I_3$53, $I_3$87, $I_3$130		C5
227.	ATP synthase beta chain, mitochondrial precursor	Q01859	59 023	6.30	S	(4)	$R_4$44, $I_4$58, $I_4$172, $I_4$319, $I_4$994, $R_3$64, $I_3$50, $I_3$163, $I_3$638		
228.	Putative ATP synthase beta chain, mitochondrial precursor	NP_916979	59 718	5.90	S	(3)	$R_4$202, $I_4$149, $I_4$154, $I_4$235, $R_3$208, $I_3$10, $I_3$61, $I_3$144		
229.	Putative ATP synthase	XP_464007	27 380	6.55	–	–	$I_4$112		
230.	F1-ATP synthase, beta subunit	CAA75477	49 219	5.25	–	–	$I_4$204		
231.	Putative NADH dehydrogenase	AAP68893	25 523	5.36	–	(2)	$I_4$780, $I_3$86, $I_3$200		
232.	Putative reductase (NADH dehydrogenase)	AAL58200	81 065	5.90	–	–	$I_4$159, $I_3$59		
233.	Putative quinone-oxidoreductase QR2	BAD03019	21 576	6.08	–	–	$R_3$101		
234.	ATP synthase F0 subunit 1	BAC19899	55 247	5.85	–	–	$R_4$77		
235.	Putative CPRD2 (a FAD binding domain pfam01565- containing protein)	BAD54133	58 898	9.34	–	–	$I_4$97		
236.	Hypothetical protein; predicted NAD/FAD-dependent oxidoreductase related protein	NP_909907	37 896	7.00	–	–	$I_4$255		

Table 2. Continued

Pr. No	Matched protein	Accession No.	MM (Da)	p*I*	SP[a)]	IN[b)]	Spots (bands) number of proteins from gels identified by MS		
							MALDI TOF MS[c)]	Nano-ESI Q-TOF MS/MS	$_{\mu}$LC Q-TOF MS/MS
	Ion transport (12)								
237.	Plasma membrane H^+-ATPase	CAD29316	94 137	5.70	–	–	$R_3$345		
238.	Putative H^+-transporting ATP synthase, highly similar to V type ATPase subunit B	NP_916591	54 246	5.03	–	(2)	$R_4$14, $I_4$492, $I_4$515, $R_3$67		
239.	Vacuolar ATPase B subunit	BAD54559	54 139	5.07	–	–	$R_4$471		
240.	Vacuolar ATPase B subunit	AAK54617	54 025	5.07	–	–	$I_4$53, $I_3$12		C5
241.	Putative vacuolar proton-ATPase, highly similar to V type ATPase catalytic subunit A	BAD27610	68 833	5.37	–	(3)	$I_4$371, $I_4$409, $I_4$541		
242.	Putative vacuolar proton-ATPase	BAD45853	68 711	5.20	–	(3)	$I_4$93, $I_4$92, $I_4$100		
243.	Porin-like protein	AAO72587	29 456	9.17	–	(2)	$I_3$43, $I_3$158		
244.	Voltage-dependent anion channel	CAC80851	29 873	7.25	–	(2)	$I_3$69, $I_3$134		
245.	Voltage-dependent anion channel	CAC80850	29 584	8.56	–	–	$I_3$30		
246.	Voltage-dependent anion channel	XP_450604	29 202	7.07	–	(2)	$I_4$532, $I_4$626		
247.	Putative voltage-dependent anion channel protein	NP_916642	33 793	5.39	–	–	$I_4$416		
248.	P0456F08.3; containing ofam00153 Mito_carrier protein domain, putative mitochondrial carrier protein	NP_916575	25 737	9.76	S	–	$R_3$198		
	Nucleotide acid metabolism (10)								
249.	Nucleoside diphosphate kinase 1	Q07661	16 851	6.30	–	–	$I_4$251, $I_3$44		
250.	Nucleoside diphosphate kinase 1	AAT70416	1635	6.3	–	–		$R_4$58	
251.	Putative nucleoside diphosphate kinase	AAV59386	26 092	8.88	–	–	$I_4$120, $R_3$124		
252.	UMP/CMP kinase A	AAF23371	23 220	5.43	–	–	$R_4$333, $R_3$21		
253.	UMP/CMP kinase A	XP_479205	23 334	5.43	–	(2)	$R_4$75, $I_4$60, $I_4$306		
254.	Adenosine kinase-like protein	AAO72629	40 206	5.57	–	–	$R_4$81, $R_3$59		
255.	Unknown protein; putative nucleoside-diphosphate-sugar epimerases	NP_910055	27 893	6.34	–	–	$R_4$434, $R_3$390		
256.	OJ1656_A11.18; putative nucleoside-diphosphate-sugar epimerases	NP_914324	44 304	5.85	–	–	$R_4$237, $R_3$172		
257.	Unknown protein; containing COG1051 domian, putative ADP-ribose pyrophosphatase	AAV44206	33 402	5.40	–	–	$I_4$207		
258.	Unknown protein; containing flavokinase domain pfam06574 and FAD synthase domain COG0196, riboflavin biosynthesis-related protein	AAO72379	38 230	6.99	S	–	$R_3$126		
	Amino acid metabolism (13)								
259.	Aspartate transaminase precursor	JC5125	47 465	7.64	S	–	$R_4$132, $I_4$72, $R_3$82, $I_3$88		
260.	Glutamine synthetase shoot isozyme	XP_467663	39 405	5.51	–	–	$R_4$280, $I_4$70, $R_3$187		
261.	OSJNBa0064H22.2; putitave glutamate decarboxylase and related PLP-dependent proteins	XP_462650	54 733	5.74	–	–		$R_4$159	
262.	Expressed protein, related to glutamine amidotransferase class II	AAT76419	26 886	5.40	–	(2)	$R_4$124, $I_4$90, $I_4$332		
263.	Putative aspartate-semialdehyde dehydrogenase	AAK63930	40 153	6.73	–	–	$R_4$247, $R_3$218		
264.	OSJNBb0038F03.5; containing GdhA domain COG0334, putative glutamate/leucine/phenylalanine/valine dehydrogenases	CAE04341	44 594	6.32	–	–	$R_4$362, $I_4$209, $R_3$270, $I_3$46		
265.	Aspartate aminotransferase	XP_463436	44 479	7.75	–	–	$R_3$179		

Table 2. Continued

Pr. No	Matched protein	Accession No.	MM (Da)	p*I*	SP[a)]	IN[b)]	Spots (bands) number of proteins from gels identified by MS		
							MALDI TOF MS[c)]	Nano-ESI Q-TOF MS/MS	$_{\mu}$LC Q-TOF MS/MS
266.	Aspartate aminotransferase	AAO23563	45 845	5.90	–	–	$R_4$243, $I_4$192, $R_3$258, $I_3$236		
267.	Putative adenosylmethionine-8-amino-7-oxononanoate aminotransferase	AAQ14479	56 439	6.33	–	2 (3)	$R_4$145, $R_4$421, $I_4$137, $I_4$463, $I_4$464, $R_3$139, $I_3$122, $I_3$220		
268.	Putative 4-methyl-5(B-hydroxyethyl)-thiazol monophosphate biosynthesis enzyme	BAD54224	42 009	5.51	–	–	$I_4$89		
269.	S-adenosylmethionine synthetase	CAC82203	43 648	5.93	–	2	$R_4$186, $R_4$194		
270.	Predicted P0487D09.8 gene product; putative glutamine synthetase	XP_507528	39 405	5.51	–	–	$R_4$131		
271.	Putative pyrroline-5-carboxylate reductase	BAC15792	29 652	7.59	–	–	–	–	C7
	Lipid metabolism (3)								
272.	Putative carboxyethylenebutenolidase (Dienelactone hydrolase)	NP_918077	30 505	6.31	–	–	$R_4$163		
273.	Putative enoyl-ACP reductase	XP_481639	39 277	8.81	–	–	$I_4$901		
274.	Putative gamma hydroxybutyrate dehydrogenase	XP_466265	30 648	6.18	–	–	$I_4$81		
	Miscellaneous (8)								
275.	OSJNBb0060M15.2; containing pfam01747 domain, putative ATP-sulfurylase	XP_471012	39 404	6.12	–	–	$I_4$129		
276.	Thioredoxin H-type (TRX-H)	XP_476912	13 319	5.16	–	–	$R_4$32		
277.	Putative isopentenyl pyrophosphate: dimethyllallyl pyrophosphate isomerase	NP_910591	27 324	4.90	–	–	$R_4$216, $R_3$325		
278.	OSJNBa0087O24.14; putative SAM dependent carboxyl methyltransferase	XP_474256	32 916	5.08	–	–	$I_4$224		
279.	Putative dihydropterin pyrophosphokinase	BAC79869	58 010	8.34	–	–	$R_3$237		
280.	Putative hydrolase	XP_462957	40 823	9.17	S	–	$R_4$256		
281.	Unnamed protein product; containing COG2072 domain, putative flavin-containing monooxygenase	XP_493782	43 850	8.62	–	–	$I_4$116		
282.	Hypothetical protein; a fusion of mitochondrial domain of unknown function pfam06449 and mitochondrial membrane protein YMF19 (OFRB) domain pfam02326	CAA76111	18 054	10.21	–	–	–	–	C12
	Unknown function proteins (35)								
283.	Hypothetical protein	AAG13425	10 546	11.00	–	–	$I_4$187, $I_3$121		
284.	Hypothetical protein	BAC79634	14 869	11.60	–	–	$R_3$188		
285.	Hypothetical protein	BAD34413	24 417	6.90	–	–	$I_4$497		
286.	Hypothetical protein	NP_920941	31 883	9.70	–	–	$R_4$288, $R_3$219		
287.	Hypothetical protein	XP_477024	17 135	10.92	–	–	$I_4$236		
288.	Hypothetical protein	BAD45444	16 871	6.96	–	–	$I_4$315		
289.	Hypothetical protein	XP_550399	64 632	5.13	–	–	$I_4$369		
290.	Hypothetical protein	NP_917969	30 035	7.64	S	–	$R_4$28		
291.	OSJNBa0044K18.17	CAE05875	40 103	7.64	–	–	$R_4$232, $R_3$169		
292.	OSJNBa0044K18.23	CAE05881	40 103	7.64	S	2	$I_3$182, $I_3$227		
293.	OSJNBa0060B20.11	XP_474907	22 113	6.23	–	–	$R_3$48		
294.	OSJNBa0088A01.18	XP_473660	116 193	9.03	–	–	$R_3$107		
295.	OSJNBa0088H09.10	XP_474414	16 880	6.08	–	–	$I_4$284, $R_3$260		
296.	OSJNBb0020O11.12	CAE04784	71 003	5.02	–	–	$R_4$435, $R_3$99		
297.	OSJNBb0058J09.11	CAD39872	15 555	5.06	–	–	$R_4$205, $R_3$133		
298.	P0018C10.6	BAC06205	8085	9.41	–	–	$I_3$105		

Table 2. Continued

Pr. No	Matched protein	Accession No.	MM (Da)	p*I*	SP[a)]	IN[b)]	Spots (bands) number of proteins from gels identified by MS		
							MALDI TOF MS[c)]	Nano-ESI Q-TOF MS/MS	$_{\mu}$LC Q-TOF MS/MS
299.	P0492F05.22	NP_913445	31 755	9.69	S	–	$R_3$578		
300.	Unknown protein	AAP50938	34 382	9.10	–	–	$I_3$196		
301.	Unknown protein	BAD36285	14 031	7.77	S	–	$R_3$100		
302.	Unknown protein	BAD36288	14 070	6.32	S	4	$R_4$9, $R_4$17, $R_4$21, $R_4$170, $R_3$381, $R_3$134, $I_4$199,		C13, C14
303.	Unknown protein	BAD36726	14 185	5.08	S	–	$R_4$60		
304.	Unknown protein	NP_919659	58 028	9.64	–	–			
305.	Unknown protein	XP_480743	24 542	5.33	S	(3)	$R_4$10, $I_4$75, $I_4$237, $I_4$212, $I_3$162		
306.	Unknown protein (pfam04784, DUF547, Protein of unknown function)	XP_470505	65 480	9.25	–	–	$R_4$103		
307.	Unknown protein	BAD53568	13 749	8.46	–	–	$R_4$143		
308.	Unknown protein	BAD03026	24 256	5.33	S	–	$R_4$147, $R_3$50		
309.	Unknown protein	BAD03882	23 442	5.45	S	–	$R_4$355, $R_3$142		
310.	Unnamed protein	NP_913551	16 662	4.78	S	–	–	$R_4$27	
311.	Unnamed protein product	NP_912762	19 341	5.93	S	–	$I_4$76		
312.	Unnamed protein product	NP_912978	39 930	7.10	–	–	$I_4$142		
313.	Unnamed protein product	NP_912984	55 309	8.14	–	–	$I_3$281		
314.	Unnamed protein product	NP_908500	43 242	11.70	–	–	$R_3$6		
315.	Unnamed protein product	NP_912944	37 592	6.08	–	–	$R_4$437, $R_3$219		
316.	Unnamed protein product	XP_469750	70 474	8.23	S	–	$R_3$223		
317.	OSJNBa0033G16.1	CAD40922	24 568	9.01	–	–	–	–	C12
	Novel proteins identified by de novo sequencing (5)								
318.	dnSP1	–	–	–	–	–	–	$R_4$4	
319.	dnSP2	–	–	–	–	–	–	$R_4$43	
320.	dnSP3	–	–	–	–	–	–	$R_4$156	
321.	dnSP4	–	–	–	–	–	–	$R_4$137	
322.	dnSP5	–	–	–	–	–	–	$R_4$3	

a) This column indicates whether the matched proteins contain signal peptides (S) or not (–), predicted by SignalP V2.0 with the score of signal peptide probability of over 0.8 caculated by Hidden Markov models.

b) This column indicates the detected isoforms which were recognized only as appeared in a gel. The numbers with or without bracket represent the isoform numbers in the PRP and PIP gel, respectively; "–" indicates no detection of isoforms.

c) This column shows the analyzed protein spots number.

R_3 and R_4 indicate that PRPs were subjected to 2-DE with pI 3–10 IEF or pI 4–7 IEF, respectively, as do I_3 and I_4. The numbers following each represents spots number on the gel.

Pr.No.: number of unique protein.

SP: signal peptide.

IN: Isoform number.

protein-enriched fraction with dithyl ether. Western blot analysis with marker proteins suggests that this fraction had no obvious contaminants from intracellular proteins (Fig. 3). To reduce the protein complexity of this fraction, the proteins were first subjected to 1-D SDS-PAGE at least 3 times to obtain reproducible protein band patterns. These separated protein bands were cut and digested and resolved by LC MS/MS (Fig. 7). When MS/MS data processed by MassLynx 3.5 were searched against the NCBInr protein sequence database by use of the MS/MS ion searching program MASCOT available on the Internet; only the proteins that matched with Mowse Score greater than 30 were accepted. Finally, we obtained 45 identities (Suppl. Table 3), of which 34 have at least 2 matched peptides, and the other 11 a single matched peptide, which were verified by further inspection of their MS/MS data according to the criteria described in Section 3.2.

This analysis resulted in the identification of 38 unique proteins (Suppl. Table 3) containing beta-1,4-xylanase and beta-glucanase, which in maize were identified as 2 major pollen coat proteins [15]. This result, in combination with Western blot data that beta-1,4-xylanase was the most abundant in the fraction with undetectable levels of plasma membrane ATPase and OsRad21-3 (Fig. 3), demonstrated

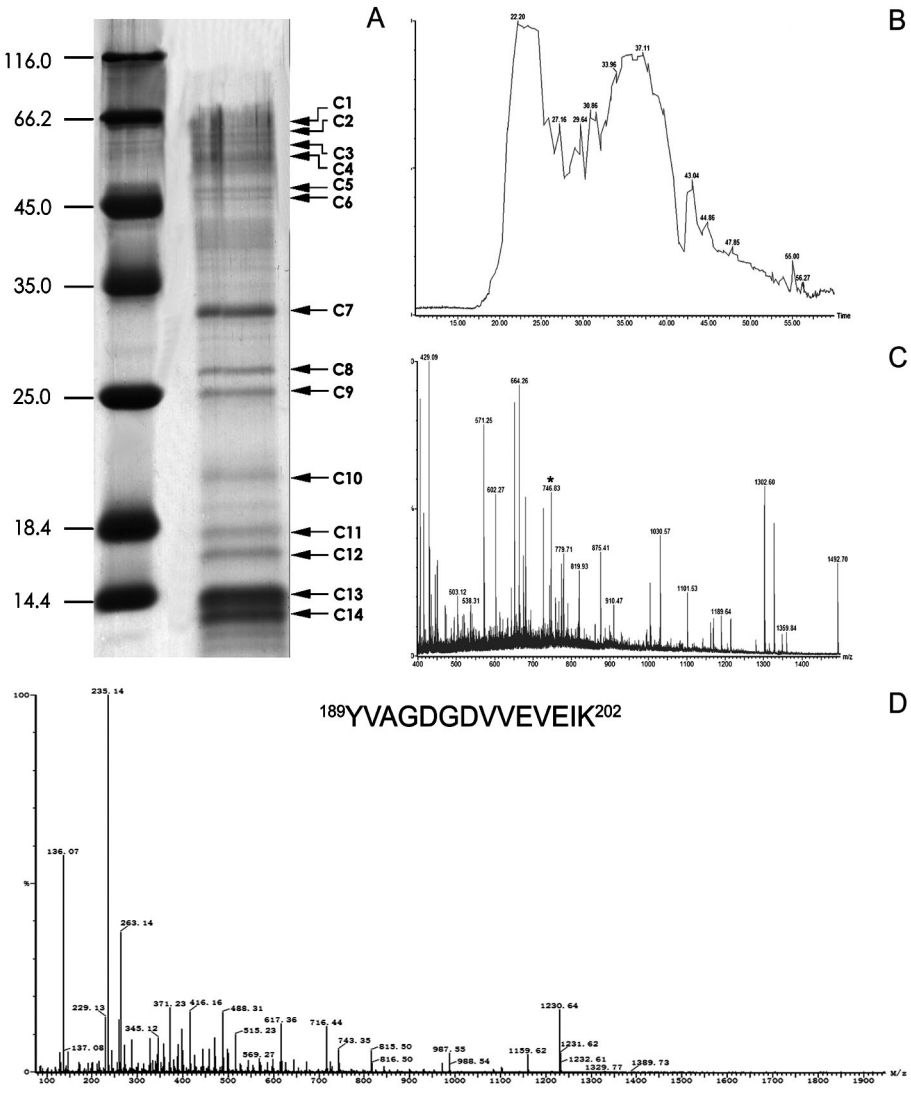

Figure 7. A representative 1-D SDS-PAGE gel pattern of the proteins extracted from mature rice pollen by dithyl ether (A), and chromatogram and MS spectra of these peptides from digested protein bands resolved by nano LC Q-TOF MS/MS (B and C).
A: 1-D SDS-PAGE pattern. 14 major bands separated by 1-D SDS-PAGE were digested and resolved by nano-LC- Q-TOF MS/MS. MM markers were co-electrophoresed in the left lane and indicated in kilodaltons. B: A representative chromatogram of the peptides from band C9 with a C18 column (75 μm × 15 cm) (see Section 2). C: the MS spectrum combined from 15 to 55 min of the gradient elution. All the peaks with double or triple charges were further analyzed by MS/MS. D: The fragmentation spectrum (MS/MS) of a doubly charged precursor ion with *m/z* 764.83 marked by asterisk in C. The spectrum was matched to a peptide, ^{189}YVAGDGDVVEVEIK^{202}, of putative expansin OsEXPB13 (AAL24476) by the internet-available MS/MS ion search program MASCOT.

that this preparation should contain the most coat-related proteins. Of them, 15 represented newly identified proteins, and the remaining 23 were overlapped with the identified PRP-derived proteins, except for 2 (vacular ATPase B subunit AAK54617 and ATP synthase alpha chain P15998), which were also present in the PIP fraction (Table 2).

3.4 Functional categories of the pollen proteins

In total, this study identified 322 unique proteins (Table 2), and among them, 75 (accounting for 23%) had more than one isoform (recognized when there was more than one isoform with p*I* and/or MM shift only in the PRP or PIP gel, as shown in Fig. 5. Furthermore, we took the MS-identified isoforms of actin (AAO38821) and tubulin (BAC82430) as examples and confirmed these MS results by Western blotting (Fig. 5).

Of the identified proteins, 242 (75%) were annotated as putative fuctional proteins, which in this study were further checked by domain search and similarity comparison, and 80 (25%) were classified in the database as unknown or hypothetical proteins. Of the unknown or hypothetical proteins, 45 proteins can be inferred a putative function on the basis of their containing conserved entire domains associated with known activities and their similarity with known proteins by PHI and PSI-BLAST search analysis (http://www.ncbi.nlm.nih). Another 35 did not contain any known conserved domains, and thus were grouped in an unknown functional protein category. Finally, this study also found 5 *de novo* proteins, for which no amino acid/nucleiotide sequence information existed in current databases (Table 1). The unknown functional proteins and *de novo* proteins represent a set of novel proteins, the identification of which presents a novel insight into the pollen protein complement.

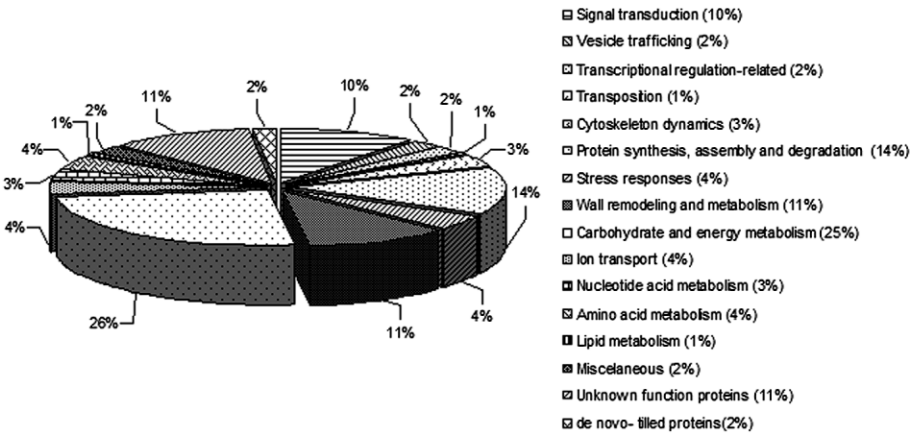

Figure 8. An outline of the functional classification of the identified proteins listed in Table 2. Each of the proteins was functionally classified based on known as well as putative functions.

From these analyses, we classified all proteins into the 16 major categories shown in Table 2 and Fig. 8. The categories included signal transduction, vesicle trafficking, transcriptional regulation-related transposition, cytoskeleton dynamics, protein synthesis, assembly and degradation, stress responses, wall remodeling and metabolism, carbohydrate and energy metabolism, ion transportation, nucleotide acid metabolism, amino acid metabolism, lipid metabolism, miscellaneous, unknown function proteins and *de novo* proteins. The major function categories are discussed below.

3.5 Signal transduction

Mature pollen might contain signaling molecules that regulate the physiological events leading to germination and cross-talk among different metabolisms, because the germination absolutely depends on the proteins presynthesized in pollen [1]. Our present study revealed 33 signal transduction-related proteins, accounting for 10% of the identified proteins. Of these, the proteins implicated in GTP-mediated signaling included 3 GDP dissociation inhibitors (GDIs), which are specifically negative regulators of GTPase activities by binding and translocating GTPases from membrane to cytoplasm [24], 3 putative GTP binding proteins and 1 beta subunit of heteromer G protein (Table 2). A previous study has indicated that GDI AAB69870, termed OsGDI1, was a functional homolog of the rab-specific GDI and able to rescue the defect in vesicle transport of budding yeast *sec19* (allelic to the GDI gene) [25]. The presence of multiple proteins related to GTPase signaling in this highly reduced tricellular organism suggests that GTPases are key regulators of pollen function.

The identified pollen-expressed Ca^{2+} sensors included 2 calreticulins, 1 putative calmodulin-like protein, and 3 C2 domain-containing proteins (Table 2). The C2 domain has been termed a Ca^{2+}-dependent phospholipid binding domain, which involves regulation of the domain-containing protein translocation between the cytoplasm and membrane by binding Ca^{2+} [26]. The pollen-expressed C2 domain-containing proteins are possible candidates functioning in cross-talk between the Ca^{2+} signal and other signal molecules. Furthermore, CIPK2 (BAA92972), a member of plant-specific serine/threonine kinase targets of calcium signals sensed and transduced by CBL proteins [27], was first identified in mature pollen. Other important protein kinases first identified in mature pollen were SnRK1b (BAC83176), a member of the SnRK1 family that plays a central role in plant sugar signaling and hormone-regulated seed development [28], and 3 other serine/threonine protein kinases (Table 2). Interestingly, this study revealed 2 WD domain-containing proteins (XP_481483 and BAD32940), of which XP_481483 was putative transforming growth factor (TGF) receptor-interacting protein and BAD32940, which is highly similar to the serine/threonine kinase receptor-associated protein NP_053629 from *M. muculus*.

Protein kinase-mediated phosphorylation-induced transitions in target protein activity requires 14-3-3 proteins, which are phosphoserine/threonine-binding proteins in both animals and plants and play key roles in cell signaling and cellular translocation of the bound partners [29]. The diversified 14-3-3 proteins (Table 2) identified in the pollen suggest the importance of the proteins in pollen functions, which is supported by previous data that a lily homolog of AAK38492 was involved in modulating PM H^+ ATPase activity during pollen germination and tube growth [30]. Furthermore, the phosphorylation-induced enzyme activity transitions are temporally regulated by dephosphorylation, which in eukaryotes is mainly catalyzed by phosphatase 2A (PP2A) [31]. Yet the holoenzyme of PP2A functions in pollen germination remains unknown because we identified only PP2A regulatory A subunit (RPA1, CAB51803), which is a scaffolding molecule to coordinate the assembly of the catalytic subunit and a variable regulatory subunit B generating functional diverse heterotrimers [31], although RPA1 is encoded by a single-copy gene in rice and capable of complementing the budding yeast mutant defective in *TPD3* encoding the PP2A A subunit [32].

Interestingly, we also identified 2 unexpected interaction module-containing proteins in the mature pollen. One was J domain pfam00226-containing putative ARG1 (NP_918662), which shared 76% overall amino acid identity to *Arabidopsis*

ARG1 involved in signal transduction of gravitropism in roots and hypocotyls [33]. Another was putative CC-NBS-LRR protein (BAC84194), which was originally identified as an important disease-resistance protein [34]. The pollen-expressed BAC84194 contains the novel NB-ARC domain pfam00931, which is considered as a module regulating protein-protein interaction in signal transduction [35]. Additionally, 3 cyclophilin-type peptidyl-prolyl *cis-trans* isomerases (PPIases) (Table 2), which in animals are important signal molecules implicated in immunosuppressive reactions [36], were also represented in the identified proteins. It is attractive to speculate whether they function in generating the invasive growth of pollen tubes in the style.

3.6 Cytoskeleton dynamics

Cytological studies have revealed that actins in mature pollen are present as large fusiform or spherical bodies [1]. The aggregates of actins are reorganized into actin filaments (AFs), first around the germination pores as pollen germination is initiated. Our identification of multiple isoforms of actin (AAO38821, Fig. 5 and Table 2) in the mature pollen conveys direct information that the presynthesied actins are necessary for initiation of germination. It is generally accepted that remodeling and dynamics of actins are directly regulated by the 3 kinds of actin-binding proteins, profilins, actin-depolymering factors (ADFs) and actin-interacting proteins (AIPs) [37, 38]. Both profilins and ADFs have been identified in the pollen of lily, *Arabidopsis* and maize [39, 40, 41], but AIP only in *Arabidopsis* pollen [37]. Our results indicated that mature rice pollen has all the 3 kinds of proteins and contained at least 1 profilin, 1 AIP and 4 different ADFs (Table 2). The newly identified pollen-expressed AIP (NP_909076) was identical to OsAIP1 (BAB21186) deduced from genomic sequence [37], on the basis of their 100% amino acid identity and grouped into a clade with *Arabidopsis* AtAIP1-1, which was able to enhance the deploymeration activities of lily ADF1 [37]. The multiple actin-binding proteins presynthesized in the mature pollen suggest that reorganization and dynamics of actins might be strictly controlled by a coordinate interaction network between these proteins, which is far from being understood now.

In contrast, although expression characterization of some tubulin-encoding genes related to pollen development has been studied [42], the function of microtubulins (MTs) in pollen germination and tube growth remains to be understood. As major components of MTs, both alpha-tubulin and beta-tubulin, which had 39% amino acid identity, were identified in mature rice pollen. The identified alpha-tubulin had 2 isotypes, and beta-tubulin was also represented by 2 isotypes (Table 2). The significance of diversified alpha- and beta-tubulin isotypes in mature pollen is still unknown. But in animal sperm, the different isotypes and translationally modified isoforms can participate in different microtubulin structure [43].

3.7 Protein synthesis, assembly and degradation

After germination is initiated, new protein synthesis with stored mRNAs presynthesized during maturation is required to support pollen tube growth [1,44]. But until now, it is unclear whether and which components of translation machinery are presynthesized in mature pollen. Here, in mature rice pollen, we identified major regulatory proteins of mitochondria and cytosol translation machinery, including 30S, 40S and 60S ribosomal proteins (Table 2), eIF4A whose homolog in mature tobacco pollen was proposed to be a possible candidate for mediating translational control in the developing male gametophyte [45], and different translational elongation factors (Table 2). Our identification also revealed 2 putative inhibitors (BAC20708 and P35681) of translation. BAC20708 is a candidate of translation initiation inhibitor. And P35681 is one of translationally controlled tumor proteins, which in animal cells are key inhibitors of protein translation elongation by acting as a guanine nucleotide dissociation inhibitor of EF1A [46] and seems to be synthesized from the stage of early young microspore development [15]. These results provide molecular evidence at the protein level that mature pollen has presynthesized the necessary components of translation machinery ready to initiate protein synthesis as entry into germination, and the protein synthesis is strictly regulated.

The function of a newly synthesized protein is determined by its correct assembly and cellular localization, both of which require molecular chaperones. The study identified multiple molecular chaperones (Table 2) representing almost all those known in other types of cells [47], including (1) 80- and 70-kDa family heat shock proteins, (2) organelle-related chaperones, (3) calreticulin (also see section 3.5) and (4) different protein disulfide isomerases (PDIs) (Table 2). Moreover, our results indicated the presence of cyclophilin-type PPIases in mature pollen (also see Section 3.5), which have been documented as molecular chaperones because of their ability to accelerating *cis-trans* isomerization of prolyl peptide bonds [36]. The mature pollen also contained putative prohibitins and putative mitochondrial processing peptidases (MPPs) (Table 2). Prohibitins from yeast and animal cells play roles in stabilizing newly synthesized mitochondially encoded proteins [48]. And MPPs in mammals and fungi are required for maturation of imported nuclear-encoded mitochondrial protein precursors [49]. The functions of the 2 new types of chaperones in plants remain unknown.

Protein degradation contributes to the regulation of protein functions especially related to highly dynamic metabolism activities occurring in germinating pollen. Our identification revealed 18 diversified proteins involved in proteolysis. Of them, 10 proteins, including 8 subunit components (Table 2) of the 26S proteasome, ubiquitin-specific protease 3 and ubiquitin-conjugating enzyme OsUBC5b (Table 2), were related to the ubiquitin/proteasome-mediated proteolysis. Two proteins, a putative Ufd1 with Ufd domain pfam03512

and a putative AAA$^+$ATPase, probably represented the 2 major components of Ufd1- AAA$^+$ATPase –Npl14 complex, which in animal cells are documented to function in activated cell matrix-associated precursors of regulatory proteins [50]. Another 6 proteins were different kinds of proteases and peptidases such as Ulp1 protease-like protein (Table 2).

3.8 Stress responses

As a highly compact tricellular organism, the pollen must obtain an ability in evolution to deal with extracellular stresses after its release from anthers and intracellular stresses caused by the active metabolism of germinating pollen and by its interaction with cells of the stigma and the style. In addition to the diversified molecular chaperones (Table 2) discussed in Section 3.7, most of them function in resistance to different intra- and extra-stresses [47], both the key enzymes involved in scavenging reactive oxygen species (ROS) [51], such as peroxiredoxin (PRX), ascorbate peroxidase (APX), superoxide dismutases (SODs), and the enzymes responsible for generating ascorbate, such as monodehydroascorbate reductase and GSH-dependent dehydroascorbate reductase, were all found in mature rice pollen (Table 2). Other identified important peroxidases involved in resistance to stress were 3 class III peroxidases (Table 2). Furthermore, 2 newly identified pollen-expressed glutathione transferases (GSTs) were classed into F type (NP_916246) and U type (T02765), respectively, and by PHI and PSI-BLAST search analysis, both of which have important roles in detoxifying toxins produced by metabolism and reducing organic hydroperoxides [52]. Therefore, our data suggest that mature pollen has a global ability to defend against biotic and abiotic stresses.

3.9 Wall remodeling and metabolism

This study identified 35 proteins, accounting for 11% of the identified proteins, involved in wall remodeling and metabolism. Of them, beta-1,4-xylanase and beta glucanase, which share more than 70% amino acid identity to each counterpart from the maize pollen coat [15], and putative glucan endo-1,3-glucosidase were possible enzymes in hydrolyzing the cereal wall-specific mixed-linked glucan. The enzyme responsible for degradation of cellulose identified here was putative cellulase.

The proteins identified here involved in pectin degradation were polygalacturonase, also identified as pollen wall-reactive proteins in maize [15], putative pectin methylesterase (PME), putative pectin methylesterase inhibitor (PMEI), putative pectin acetylesterase (PAE) and putative esterase D (Table 2). PME identified first in cereal pollen by this study and previously reported only in tobacco pollen [53] has been recognized as an important enzyme to regulate cell wall loosening in diversified vegetative tissues by catalyzing demethylesterification of homogalacturonans, major components of pectins [54]. PMEI, originally discovered in kiwi fruit [55] and recently reported in maize pollen [15], has been proposed to be a major regulator of PME activity. The pollen-expressed PAE has the active site GxSxG present in *Erwinia chrysanthemi* 39937 PAE, which has the activity for deacetylation of esterified oligogalacturides [56], and the pollen-expressed esterase D is related to the Pfam00756 family, which acts on carboxylic esters. Thus, this study provides the first evidence that mature pollen of cereals has multiple enzymes involved in the regulation of pectin degradation, which suggests that pectins have important roles in pollination and fertilization of cereals, although some previous studies indicated that pectins were abundant in dicot cell walls but less so in cell walls of cereals [56]. Furthermore, 2 beta-galactosidases (Table 2) we identified have the active site-containing consensus sequence GGP[LIVM]xQENE[FY] conserved in the known β-galactosidases from bacteria, mammals and plant fruit, which catalyze the hydrolysis of terminal galactosyl residues from different components of the cell and/or cell wall [57].

The identified wall-loosening/expansing proteins included 4 beta-expansins (Table 2), which are presumed to play roles in loosening cell walls of the stigma and transmitting tract of the style [11,15]; pollen allergen Ory s1, which was reported previously as a major allergen of rice pollen and now recognized as a subgroup of beta-expansin [58]; and 4 12-kDa pollen allergens (Table 2), which were identified as beta-expansin-like proteins. The putative pollen-specific protein C13 (BAD54680) was identified as an extensin-like allergen. Three class III peroxidases (Table 2), known to be involved in cell elongation, wall construction and differentiation besides playing roles in the defense against pathogens (also see section 3.8) [59], were also identified.

Furthermore, pollen wall dynamics in tube growth requires active wall synthesis. The proteins implicated in the process we newly identified in pollen were UDP-glucose pyrophosphorylase discussed in section 3.10, GDP-mannose pyrophosphorylase, UDP-glucuronic acid decarboxylase, putative myo-inositol-1-P synthase, putative myo-inositol monophosphatase, reversibly glycosylated polypeptides (RGPs) and cellulose synthase-like F7 (OsCslF7), a member of the cereal-specific cellulose synthase-like family [60] (Table 2). GDP-mannose pyrophosphorylase and UDP-glucuronic acid decarboxylase are critical enzymes to catalyze Mannose-1-P to UDP-xylose, which is further used for glycoprotein and polysaccharide synthesis [61, 62]. Myo-inositol-1-P synthase and myo-inositol monophosphatase are responsible for synthesis of myo-inositol-1-P and free myo-Inositol, which is further utilized for cell membrane and wall biosynthesis [63]. RGPs identified originally in pea seedlings have been recognized to be responsible for delivering nucleotide sugars from the cytosol to the Golgi surface, where the sugars are used for synthesizing polysaccharide molecules [64].

3.10 Carbohydrate and energy metabolism

Starch is preferentially stored in mature cereal pollen as energy-/carbon skeleton-containing materials to support pollen functions. Our results indicated that the enzymes involved in the processes were highly represented, accounting for 25% of the identified proteins. This result helps in understanding how starch in pollen is broken down and further metabolized during germination.

The newly identified pollen-expressed debranching enzyme, α-amylase, and α-1,4-glucan phosphorylase (Table 2) suggests that starch in pollen is hydrolyzed by the pathway similar to that in germinating rice seeds [65]. The key enzyme, vacuolar invertase, responsible for hydrolysis of sucrose into free glucose and fructose, were identified in mature rice pollen as 2 different types (AAF87245 and AAF87246) with 62% amino acid identity. AAF87245 was found to accumulate in rice anthers just before the heading stage [11]. As well, hexokinase and/or fructokinase, both identified in this study (Table 2), function in catalyzing the 2 free hexoses to enter the hexose phosphate pool consisting of glucose-1-phosphate, glucose-6-phosphate and fructose-6-phosphate. And the dynamic equilibrium of the hexose pool is kept by the action of phosphoglucomutase and phosphoglucose isomerase, both found in mature rice pollen (Table 2).

In the nonphotosynthetic organism, the hexose phosphate pool is mainly drained for further carbohydrate metabolism. This study identified most enzymes involved in glycolysis and tricarboxylic acid (TCA) cycle (Table 2), which included the key enzymes in glycolysis such as fructose biphosphate adolase and triose phosphate isomerase (Table 2) and the key enzymes catalyzing pyruvate into TCA cycle, such as dihydrolipoamide acetyltransferase, dihydrolipoamide dehydrogenase and citrate synthase (Table 2). Our results also indicated the presence of the key enzymes (such as 6-phosphogluconolactonase, Table 2) involved in pentose phosphate pathway in the mature pollen. Interestingly, mature rice pollen contained alcohol dehydrogenase (AAF34414), one of the key enzymes dedicated to ethanolic fermentation. The multiple pathways occurred in pollen are consistent with active protein synthesis and vesicle transport in germinating pollen to support the tube advance.

When the hexose phosphate pool is utilized for the biosynthesis of cell wall polysaccharides, glucose-1-phosphate is first converted to UDP-glucose (UDPG) by UDP-glucose pyrophosphorylase, which was identified in the pollen with multiple isoforms (Table 2, also see Section 3.9), and UDPG is the direct substrate of cellulose and noncellulose polysaccharides.

4 Concluding remarks

Pollen grains, which are highly desiccated and thus metabolically quiescent when released from anthers of diploid plants [66], can initiate germination and polar tube growth within minutes of pollination on stigmas. But the molecular mechanism underlying the process is poorly understood because of lack of pollen protein information [12]. In this study, we identified 322 unique proteins from the mature rice pollen using proteomic approaches. Based on our present knowledge, these proteins, however representing only a part of the pollen protein complement, were at least associated with 14 distinct metabolism pathways involved in pollen functions. Our results provide the first direct evidence for the notion that pollen germination depends on the presynthezed proteins in mature pollen [1].

Besides the proteins implicated in carbohydrate and energy metabolism, which are considered a basis of pollen functions, the overrepresentation of the proteins related to signal transduction, wall remodeling and metabolism, and protein synthesis, assembly and degradation, accounting for 35% of the identified proteins, suggests that the 3 kinds of metabolism play vital roles in the functional specialization of pollen. This conclusion is supported in part by a recent result that transcripts encoding proteins implicated in wall metabolism, signaling and cytoskeleton were overrepresented in the Arabidopsis pollen transcriptome [8]. But the transcriptomic analysis cannot reveal the importance of the metabolism of protein synthesis, assembly and degradation in pollen functions, mainly because these transcripts encoding proteins implicated in this metabolism, at least some of them, are undetectable in mature pollen [7]. Our present study, combined with previous biochemical analysis [1], clearly indicated that this set of proteins have been presynthesized during pollen maturation.

Meanwhile, our results also yield other novel insights into pollen functions: (1) that 23% of the unique proteins had isoforms suggests that PTM may be an important way to diversify the function of a protein in the haploid genome; (2) pollen has presynthesized multiple molecular chaperones and antioxidant proteins during the mature stage to handle abruptly metabolic changes during normal germination; and (3) pectin may play important roles in pollen tube polar growth and fertilization of monocots because major enzymes involved in pectin metabolism were identified first in this study. Furthermore, the identified pollen-expressed unknown functional proteins, accounting for 11% of the identified proteins and the *de novo*-identified proteins may represent a set of novel proteins. Thus, our study provides the first close investigation, to our knowledge, of the protein complement of mature pollen and useful molecular information to further understand pollen functions. However, it is obvious that the identified proteins only represent a small set of pollen-expressed proteins. Further experiments including the identification of interaction networks based on the identified important proteins, and proteomic analysis of subcellular compartments will be necessary to understand the mechanisms underlying pollen functions.

The proteome analysis facility in Institute of Botany, Chinese Academy of Sciences (IBCAS) was established under the CAS proteome research program. We acknowledge Xiaohong Qian, Jie

Wang and Hongxia Wang (China National Center of Biomedical Analysis) and Siqi Liu and Jingqiang Wang (Beijing Genomics Institute, Chinese Academy of Sciences) for their technical assistance in MS analyses and helpful discussion during preparation and revision of this manuscript. We thank Ming Yuan (China University of Agriculture) for his help in preparation of the TEM samples. The antibodies against maize pollen coat-specific beta-1,4-xylanase and plasma membrane H^+-ATPase PMA2 from Nicotiana plumbaginifolia were a gift from Anthony Huang (University of California at Riverside, USA) and Marc Boutry (University of Louvain, Belgium). Specially, we also thank the reviewers for their critical reading of this manuscript. This research was supported by CAS (grant No. KSCX-SW-307), IBCAS and the Ministry of Science and Technology (grant No. 2005CB120804).

5 References

[1] Mascarenhas, J. P., *Plant Cell* 1993, *5*, 1303–1314.

[2] Franklin-Tong, V. E., *Curr. Opin. Plant Biol.* 2002, *5*, 14–18.

[3] Lord, E. M., Russell, S. D., *Annu. Rev. Cell Dev. Biol.* 2002, *18*, 81–105.

[4] Qiao, H., Wang, H., Zhao, L., Zhou, J. *et al.*, *Plant Cell* 2004, *16*, 582–595.

[5] Li, H., Lin, Y. K., Heath, R. M., Zhu, M. X. *et al.*, *Plant Cell* 1999, *11*, 1731–1742.

[6] Fu, Y., Wu, G., Yang, Z., *J. Cell Biol.* 2001, *152*, 1019–1032.

[7] Becker, J. D., Boavida, L. C., Carneiro, J., Haury, M. *et al.*, *Plant Physiol.* 2003, *133*, 713–725.

[8] Honys, D, Twell, D., *Plant Physiol.* 2003, *132*, 640–652.

[9] Lockhart, D. J., Winzeler, E. A., *Nature* 2000, *405*, 827–836.

[10] Mayfield, J. A., Fiebig, A., Johnstone, S. E., Preuss, D., *Science* 2001, *292*, 2482–2485.

[11] Kerim, T., Imin, N., Weinman, J. J., Rolfe, B. G., *Proteomics* 2003, *3*, 738–751.

[12] McCormick, S., *Plant Cell* 2004, *16*, S142–S153.

[13] Bradford, M. M., *Anal. Biochem.* 1976, *72*, 248–254.

[14] Song, Z. P., Lu, B. R., Chen, J. K., *Int. Rice Res. Notes* 2001, *26*, 31–32.

[15] Suen, D. F., Wu, S. S., Chang, H. C., Dhugga, K. S. *et al.*, *J. Biol. Chem.* 2003, *278*, 43672–43681.

[16] Fu, J. H., Lei, L. G., Chen, L. B., Qiu, G. Z., *Aust. J. Bot.* 2001, *49*, 771–776.

[17] Morsomme, P., Dambly S., Maudoux O., Boutry M., *J. Biol. Chem.* 1998, *273*, 34837–34842.

[18] Zhang, L. R., Tao, J.Y., Wang, T., *J. Exp. Bot.*, 2004, *5*, 1149–1152.

[19] Yokota, E., Ohmori, T., Muto, S., *Planta* 2004, *218*, 1008–1018.

[20] Lenartowska, M., Karas, K., Karshall, J., Napier, R. *et al.*, *Protoplasm* 2002, *219*, 23–30.

[21] Boudart, G., Jamet, E., Rossignol, M., Lafitte, C. *et al.*, *Proteomics* 2005, *5*, 212–225.

[22] Pitarch, A., Sanchez, M., Nombela, C., Gil, C., *Mol. Cell. Proteomics* 2002, *1*, 967–982.

[23] Chivasa, S., Ndimba, B. K., Simon, W. J., Robertson, D. *et al.*, *Electrophoresis* 2002, *23*, 1754–1765.

[24] Sasaki, T., Takai, Y., *Biochem. Biophys. Res. Commun.* 1998, *245*, 641–645.

[25] Kim, W. Y., Kim, C. Y., Cheong, N. E., Choi, Y. O. *et al.*, *Planta* 1999, *210*, 143–149.

[26] Rizo, J., Sudhof, T. C., *J. Biol. Chem.* 1998, *273*, 15879–15882.

[27] Kolukisaoglu, Ü., Weinl, S., Blazevic, D., Batistic, O. *et al.*, *Plant Physiol.* 2004, *134*, 43–58.

[28] Rolland, F., Moore, B., Sheen, J., *Plant Cell* 2002, *14*, S185–S205.

[29] Roberts, M. R., *Trends Plant Sci.* 2003, *8*, 218–223.

[30] Pertl, H., Himly, M., Gehwolf, R., Kriechbaumer, R. *et al.*, *Planta* 2001, *213*, 132–141.

[31] Janssens, V., Goris, J., *Biochem. J.* 2001, *353*, 417–439.

[32] Yu, S., Lei, H., Chang, W., Soll, D. *et al.*, *Plant Mol. Biol.* 2001, *45*, 107–112.

[33] Sedbrook, J. C., Chen, R., Masson, P. H., *Proc. Natl. Acad. Sci. USA* 1999, *96*, 1140–1145.

[34] Meyers, B. C., Kozik, A., Griego, A., Kuang, H. *et al.*, *Plant Cell* 2003, *15*, 809–834.

[35] van der Biezen, E. A., Jones, J. D., *Curr. Biol.* 1998, *8*, R226–R227.

[36] Harrar, Y., Bellini, C., Faure, J. D., *Trends Plant Sci.* 2001, *6*, 426–431.

[37] Allwood, E. G., Anthony, R. G., Smertenko, A. P., Reichelt, S. *et al.*, *Plant Cell* 2002, *14*, 2915–2927.

[38] Chen, C. Y., Cheung, A. Y., Wu, H. M., *Plant Cell* 2003, *15*, 237–249.

[39] Chung,Y. Y., Magnuson, N. S., An, G. H., *Mol. Cells*, 1995, *5*, 224–229.

[40] Lopez, I., Anthony, R. G., Maciver, S. K., Jiang, C. J. *et al.*, *Proc. Natl. Acad. Sci. USA* 1996, *93*, 7415–7420.

[41] Vidali, L., Hepler, P. K., *Cell Motil. Cytoskel.* 1997, *36*, 323–338.

[42] Cheng, Z., Snustad, D. P., Carter, J. V., *Plant Mol. Biol.* 2001, *147*, 389–398.

[43] Kierszenbaum, A. L., *Mol. Reprod. Dev.* 2002, *62*, 1–3.

[44] Taylor, L. P., Hepler, P. K., *Annu. Rev. Plant Physiol. Plant Mol. Biol.* 1997, *48*, 461–491.

[45] den Camp, R. G. L., Kuhlemeier, C., *Nucl. Acids Res.* 1998, *26*, 2058–2062.

[46] Cans, C., Passer, B. J., Shalak, V., Nancy-Portebois, V. *et al.*, *Proc. Natl. Acad. Sci. USA* 2003, *100*, 13892–13897.

[47] Miernyk, J. A., *Plant Physiol.* 1999, *121*, 695–703.

[48] Nadimpalli, R., Yalpani, N., Johal, G. S., Simmons, C. R., *J. Biol. Chem.* 2000, *275*, 29579–29586.

[49] Kitada, S., Yamasaki, E., Kojima, K., Ito, A., *J. Biol. Chem.* 2003, *278*, 1879–1885.

[50] Ye, Y., Meyer, H. H., Rapoport, T. A., *J. Cell Biol.* 2003, *162*, 71–84.

[51] Dietz, K. J., *Plant Mol. Biol.* 2003, *54*, 93–107.

[52] Dixon, D. P., Lapthorn, A., Edwards, R., *Genome Biol.* 2002, *3*, R3004.1–R3004.10.

[53] Li, Y. Q., Mareck, A., Faleri, C., Moscatelli, A. *et al.*, *Planta* 2002, *214*, 734–740.

[54] Micheli, F., *Trends Plant Sci.* 2001, *6*, 414–419.

[55] Balestrieri, C., Castaldo, D., Giovane, A., Quagliuolo, L. *et al.*, *Eur. J. Biochem.* 1990, *193*, 183–187.

[56] Shevchik, V. E., Hugouvieux-Cotte-Pattat, N., *J. Bacteriol.* 2003, *185*, 3091–3100.

[57] Smith, D. L., Gross, K. C., *Plant Physiol.* 2000, *123*, 1173–1184.

[58] Cosgrove, D. J., Bedinger, P., Durachko, D. M., *Proc. Natl. Acad. Sci. USA* 1997, *94*, 6559–6564.

[59] Passardi, F., Longet, D., Penel, C., Dunand, C., *Phytochem.*, 2004, *65*, 1879–1893.

[60] Hazen, S. P., Scott-Craig, J. S., Walton, J. D., *Plant Physiol.*, 2002, *128*, 336–340.

[61] Conklin, P. L., Norris, S. R., Wheeler, G. L., Williams, E. H. *et al.*, *Proc. Natl. Acad. Sci. USA* 1999, *96*, 4198–4203.

[62] Harper, A. D., Bar-Peled, M., *Plant Physiol.* 2002, *130*, 2188–2198.

[63] Loewus, F. A., Murthy, P. P. N., *Plant Sci.* 2000, *150*, 1–19.

[64] Saxena, I. M., Brown, Jr.R. M., *Trends Plant Sci.* 1999, *4*, 6–7.

[65] Koller, A., Washburn, M. P., Lange, B. M., Andon, N. L. *et al.*, *Proc. Natl. Acad. Sci. USA* 2002, *99*, 11969–11974.

[66] Edlund, A. F., Swanson, R., Preuss, D., *Plant Cell* 2004, *16*, S84–97.

